Characterization of the Mechanistic Roles of Rif1-Glc7 in DNA Double-Strand Break Repair Pathway Choice in *Saccharomyces cerevisiae*

by

Rebecca Quinn

A thesis

presented to the University of Waterloo

in fulfillment of the

thesis requirement for the degree of

Master of Science

in

Biology

Waterloo, Ontario, Canada, 2023

AUTHOR'S DECLARATION

I hereby declare that I am the sole author of this thesis. This is a true copy of the thesis, including any required final revisions, as accepted by my examiners.

I understand that my thesis may be made electronically available to the public.

Abstract

Rap-1 interacting factor 1 (Rif1) is a protein involved in telomere regulation, DNA replication and has more recently been found to mediate genomic stability by influencing the choice of DNA double-strand break (DSB) repair pathway. Rif1 and protein phosphatase 1 (PP1, Glc7 in budding yeast) prevent premature DNA replication initiation by maintaining dephosphorylation of the Mcm2-7 helicase, ensuring it remains inactive. Dbf4-dependent kinase (DDK) can counteract this at the onset of S phase by binding and phosphorylating Rif1 to prevent its interaction with PP1. It has recently been shown that Rif1 may similarly target PP1 to affect DSB repair pathway choice. However, the precise mechanisms involved remain unclear.

To examine the importance of the interaction between Rif1 and Glc7 in determining DNA DSB repair pathway choice, a *rif1 5AΔPPDSPP* mutant has been created by deleting the Dbf4 binding motif on Rif1 (PPDSPP), which allows DDK to phosphorylate Rif1, and by mutating 5 cyclin-dependent kinase (CDK) phosphorylation sites to alanine (5A), located near the Glc7-binding site. Thus, this Rif1 mutant is not expected to be phosphorylated by DDK nor CDK, allowing Rif1-Glc7 to be constitutively active, resulting in an increase in Rif1-mediated Glc7 dephosphorylation activity. We find that this mutant is hypersensitive to DNA DSB-inducing agents and this sensitivity is partially rescued by abrogating the interaction between Rif1 and Glc7 through its conserved RVxF/SILK motifs. Partial rescue is additionally observed when Rif1 is unable to translocate to the inner nuclear membrane or bind to DNA ends at the DSB. Furthermore, upon DSB induction, less resection can be

observed in this mutant strain, suggesting repair by the non-homologous end-joining (NHEJ) pathway. Through a series of experiments, this work demonstrates a role of Rif1 and Glc7, in the context of DNA DSBs, to promote repair by NHEJ.

Acknowledgements

Firstly, I would like to express my gratitude to my supervisor, Dr. Bernard Duncker. I would not be the scientist I am today without your consistent mentorship and demonstration of what it means to be a true researcher. Working in your lab was both challenging and rewarding, and pushed me to become a more resilient, inquisitive individual. Thank you for your guidance and expertise throughout my time in the Duncker lab. Thank you to Dr. Moira Glerum and Dr. Andrew Doxey for being on my committee and providing me with valuable feedback in my masters. Thank you to the faculty of the Department of Biology and my wonderful course instructors, Dr. Scott Leatherdale and Dr. Moira Glerum, for contributing to my experience and degree at the University of Waterloo. Thank you to all of my students whom I had the pleasure of being a TA for in BIOL240L, BIOL120L, and BIOL130L. You all contributed to making my time in my master's fun and engaging.

I would also like to show my appreciation to the Duncker lab members who played an integral role in my time in the lab. Thank you to Manaswi Sharma and Karan Patel for your help on these projects and allowing me to be your mentor for your 499 courses. Dr. Muneera Fayyad, thank you for being my first mentor and taking me under your wing from day 1. Your support and friendship are two things I will always cherish. I would like to thank Geburah Straker for your willingness to always help and offer your expertise, as well as for being so open with me on your past experiences. Thank you to Mike Meleka and Anthony Dang for consistently supporting me. You both never failed to brighten my day and I will be forever grateful for our long days and late nights in the lab, the laughs, the bubble tea, the

problem solving together, and, ultimately, for what I hope is a life-long friendship. I am excited to see where your futures take you.

Lastly, I'd like to thank my family. To my mom, Jen, my dad, Edd, and my brother, Nick, your unconditional love and support means the world to me. While you may have not been able to understand my work in the lab, you supported me nonetheless and celebrated with me as if they were your CRISPR mutations that worked! Thank you for raising me into the woman I am today.

Table of Contents

List of Figures

List of Tables

List of Abbreviations

CDC: Cell division cycle

CDK: Cyclin-dependent kinase

CMG: Cdc45, Mcm2-7, GINS

DDK: Dbf4-dependent kinase

DDR: DNA damage response

DNA: Deoxyribonucleic acid

DSB: Double strand break

dsDNA: double-stranded DNA

EDTA: Ethylenediaminetetraacetic acid

FL: Full-length

GINS: Go-Ichi-Ni-San

gRNA: guide RNA

HR: Homologous recombination

HU: Hydroxyurea

LB: Lysogeny broth

MCM: Minichromosome maintenance

MRN: Mre11-Rad50-Nbs1

MRX: Mre11-Rad50-Xrs2

MYC: Myelocytamatosis

NHEJ: Non-homologous end-joining

ORC: Origin recognition complex

PCR: Polymerase chain reaction

PIPs: PP1-interacting proteins

Pre-IC: Pre-initiation complex

Pre-LC: Pre-loading complex

Pre-RC: Pre-replicative complex

SC: Synthetic complete

sgRNA: single-guide RNA

ssDNA: single-stranded DNA

UV: Ultraviolet

WT: Wild-type

YPD: Yeast extract, peptone, dextrose

Chapter 1

Introduction

1.1 Background

1.1.1 *Saccharomyces cerevisiae* as a Model Organism

The budding yeast, *Saccharomyces cerevisiae*, is a desirable model organism in the world of biological research. Its easily manipulated, well-researched genome, rapid growth rate, and conservation of many molecular processes between mammalian and yeast cells represent some of the various reasons why *S. cerevisiae* is an ideal candidate for researchers to conduct their studies with (Mohammedi, *et al*., 2015; Fukuhara, *et al*., 2010). First experimented with in the 1930s by Øjvind Winge and Carl Lindegren, the model organism has been used in a plethora of publications, contributing to the understanding of human disease and molecular interactions (Burgess *et al*., 2017; Duina *et al*., 2014). Another popular use of budding yeast is attributable to its ability to ferment sugars into alcohol, making it a cheap and quick way to produce beer. The yeast fermentation process also creates carbon dioxide, serving as a useful leavening agent in the production of bread. This facultative anaerobe grows well in environments with or without oxygen, given that it has glucose to breakdown to then perform aerobic respiration or anaerobic fermentation, respectively (Gasmi *et al*., 2014).

Another unique characteristic of *S. cerevisiae* is its reproduction method – budding. Budding occurs when a mother cell creates a protrusion of itself, the “bud”, that eventually pinches off to become a daughter cell. This daughter cell is a genetically identical copy of the mother, and this division can occur every 90 minutes in a laboratory setting, making budding

yeast a useful model organism (Duina *et al*., 2014). While budding is an asexual process, yeast cells can also reproduce sexually undergoing meiosis via haplo-selfing (Knop, 2006). Haploid cells of opposite mating type, MATa or MATα, can join together to create a diploid zygote, undergo meiosis, and produce 4 gametes. While budding is the predominant method of reproduction in this yeast, as per its name "budding yeast", sexual reproduction is crucial for its survival outside of laboratory settings, as it allows for genetic diversity. This type of reproduction is also useful for research, as the HO gene can be put under an inducible promoter, which will perform a double-strand break (DSB) at the mating type locus once transcribed and translated to the HO endonuclease. Therefore, researchers can take advantage of this natural system to induce DSBs for experiments, such as resection assays.

The advantage of using budding yeast in scientific experiments dramatically increased upon the sequencing of its genome, as a result of the work of Goffeau *et al*., 1996. They identified 6000 genes, consisting of both prokaryotic origin, as a result of lateral gene transfer, and, primarily, eukaryotic origin, and of which 5570 encode for proteins (Wood *et al*., 2001; Hall *et al*., 2005; Parapouli *et al*., 2020). Remarkably, 23% of genes in this single-cell organism have human homologues, making it highly relevant for studying and contributing to the understanding of human cellular processes (Jiang *et al*., 2008; Liu *et al*., 2017). Some of its diverse research implications include better understanding the cell cycle, DNA damage response, aging, epigenetic regulation, apoptosis, and infectious diseases (Glingston *et al*., 2021; Karathia *et al*., 2011; Ramotar & Masson, 1996).

1.1.2 Cell Cycle of *S. cerevisiae*

The cell cycle of budding yeast allows the organism to grow and divide, duplicating its genome and producing either diploid or haploid cells. Typically, *S. cerevisiae* replicates via budding and, thus, this is the cell cycle that is described. The cell cycle can be divided into 4 stages: Gap 1 (G1) phase, when the cell prepares for replication of its DNA; Synthesis (S) phase, when DNA replication occurs; Gap 2 (G2) phase, when the cell prepares for mitosis; and Mitosis (M) phase, when mitosis occurs. There are also two major checkpoints: the G1 checkpoint and the spindle assembly checkpoint. The purpose of cell cycle checkpoints is to ensure the cell does not advance a stage prematurely before faithfully completing a previous one (Lew & Reed, 1995). Cyclin-dependent kinases (CDKs), and cyclins regulate and arrest the cell cycle if DNA damage is sensed at either checkpoint. In yeast, there is only one CDK, Cdc28, and there are nine cyclins which can bind Cdc28 to form complexes and regulate its function (Enserink, 2011). The inactivation of Cdc28 has been found to prevent cell cycle arrest, allowing cells with DNA damage to enter mitosis and undergo nuclear division (Li & Cai, 1997). It is therefore essential that Cdc28 maintains its role throughout the cell cycle, as well as form complexes with the correct cyclins at the right time. When Cdc28 complexes with a cyclin, it can phosphorylate proteins resulting in the activation or inactivation of the substrate, influencing the cell cycle and other processes.

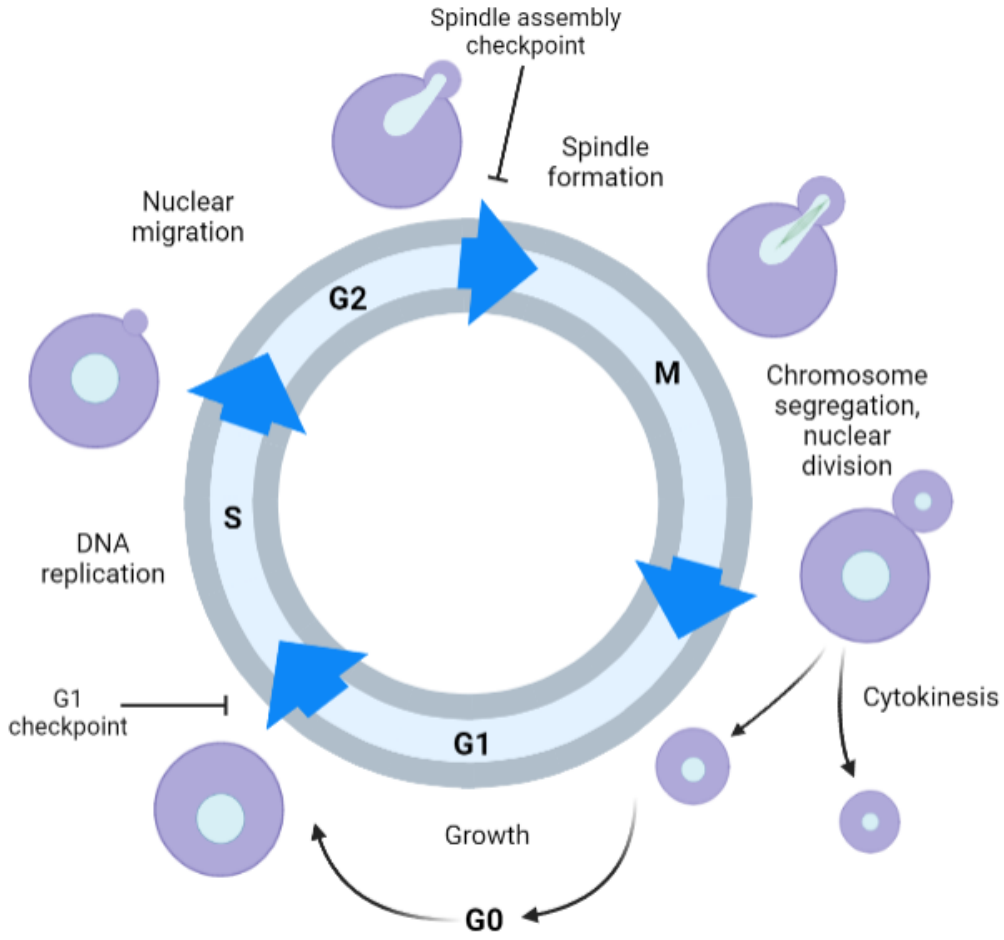

Figure 1.1 Overview of *S. cerevisiae* cell cycle. The four stages of the budding yeast cycle, along with the major checkpoints. The cell cycle progresses as such: Gap 1 (G1) phase, Synthesis (S) phase, Gap 2 (G2) phase, and Mitosis (M) phase. Cells can remain dormant in quiescence (G0), where they do not undergo proliferative growth.

1.1.3 DNA Replication Initiation

DNA replication is a tightly controlled process in the cell cycle that consists of 3 main stages: initiation, elongation, and termination. At the beginning of G1 phase, cyclin levels are low while the cell continues to grow and prepare for S phase. As G1 progresses, cyclin Cln3 forms a complex with Cdc28 and phosphorylates Whi5 (Costanzo *et al*., 2004; de Bruin *et al*., 2004). This acts as a safeguard to prevent premature entry of cells into S phase. Cyclins, Cln1 and Cln2, also increase in mid-G1 phase, allowing cells to progress through the start-transition (START). Once the cell goes through START, the cell must complete the cell cycle, making the G1 checkpoint essential for ensuring that DNA damage is repaired before the cell duplicates its chromosomes in S phase. If cells are not ready to commit to this process, they can remain dormant in quiescence (G0), which is the predominant state of all cells, unless cells are undergoing proliferation and division (O'Farrell, 2011; Valcourt *et al*., 2012; Sun & Gresham, 2021).

In late G1 phase, specific loci in the genome, known as origins of replication, are where initiation begins and recruit a variety of factors to form the pre-replicative complex (pre-RC) (Li & Stillman, 2013; Leonard & Mechali, 2013). The first step requires the binding of the origin recognition complex (ORC), which is followed by Cdc6 binding, a loading factor (Leonard & Mechali, 2013). The Mcm2-7 helicase then binds with Cdt1 to complete the pre-RC, which is activated by CDK and Dbf4-dependent kinase (DDK) at the end of G1 phase (Frigola *et al*.,

2013). After the licensing and activation of origins via CDK and DDK, origin firing can occur marking the beginning of S phase (Jackson *et al*., 1993).

In late G1 phase/early S phase, the cyclins, Clb5 and Clb6, increase in abundance and support cell proliferation (DeCesare & Stuart, 2012). Simultaneously, levels of DDK's regulatory subunit, Dbf4, begin to rise and at the onset of S phase, there is a spike in DDK activity. DDK alleviates an inhibitory effect of the of Mcm4 N terminus, part of the Mcm2-7 helicase, through phosphorylation (Sheu & Stillman, 2010). Furthermore, the pre-loading complex (pre-LC) begins to form after CDK-meditated phosphorylation of Sld2 and Sld3, eventually leading to a complex of Dpb11, GINS, Sld2 and DNA polymerase ε (Tanaka *et al*., 2007; Zegerman & Diffley, 2007). The pre-initiation complex (pre-IC) proceeds from the pre-LC, and the replacement of Sld3 with GINS leads to the formation of the CMG helicase, comprised of Cdc45, Mcm2-7 and GINS (Moyer *et al*., 2006; Bruck & Kaplan, 2011). The CMG helicase then unwinds the DNA bidirectionally for replication to ensue and the replisome, a complex consisting of CMG helicase, DNA polymerase, and accessory proteins, can carry out DNA replication (Seo & Kang, 2018). DNA polymerase synthesizes the DNA in a 5' to 3' direction, where one strand is the leading strand, growing continuously, and the other strand is the lagging strand, generating Okazaki fragments (Okazaki *et al*., 1968). Okazaki fragments are synthesized between RNA primers and are joined together by DNA ligase after removal of the primers by an exonuclease. DNA replication termination occurs when two forks merge and replisomes collide. Once S phase is complete and the 16 chromosomes in budding yeast have been successfully duplicated, cells can enter M phase and begin to undergo mitosis.

1.2 DNA Double-Strand Break Repair

In eukaryotes, there are two main DSB repair pathway choices, the error-prone non-homologous end joining (NHEJ) pathway, and the more precise homologous recombination (HR) pathway. NHEJ occurs predominantly in G1 phase, but can transpire at any point in the cell cycle, whereas HR takes place in S or G2 phase (Mao *et al*., 2008; Fugger & West, 2016). While HR is the preferred method of repair in yeast, NHEJ is predominant in human cells. In both instances, the MRX complex (MRN in mammalian cells) and the Ku70/80 ring heterodimer are recruited to the DNA ends (Chapman *et al*., 2012).

If NHEJ is chosen as the pathway to repair the DSB, Nej1 is recruited to the break to aid in the stability of the Ku complex and to regulate the activity of the DNA ligase complex, Dnl4-Lif1 (Yang *et al*., 2015) (figure 1.2.1). Alternatively, when Sae2 (CtIP in mammalian cells) is recruited and phosphorylated by CDK, other end-processing factors, such as Exo1 and Sgs1-Dna2 are recruited and begin the processing of DSB ends, resulting in the HR pathway (Gobbini *et al*., 2016). These proteins aid in bidirectional processing, removal of the Ku complex and leave long stretches of ssDNA overhangs at the 3’ ends (Chanut *et al*., 2016; Gobbini *et al*., 2016). Replication protein A (RPA) stabilizes the ssDNA overhangs and is eventually replaced by Rad51 upon invasion of the homologous template (Ma *et al*., 2017).

The repair pathway that is chosen depends on a variety of factors. Depending on the cause of the DSB, different repair pathways are preferred. For example, if the topoisomerase II (topII) inhibitor, etoposide, is given to yeast cells, which works by binding to topII and

preventing the re-ligation of the DNA DSB ends, most of the breaks will be repaired via HR (Sabourin *et al.*, 2003). In general, the NHEJ pathway is less preferred to repair yeast DNA DSBs in comparison to mammalian DSBs. However, NHEJ may be used as a back-up for HR when this pathway is blocked in yeast cells (Takata *et al.*, 1998). Repair pathway choice is essential to a cell's survival, and both pathways offer their own unique sets of advantages and disadvantages.

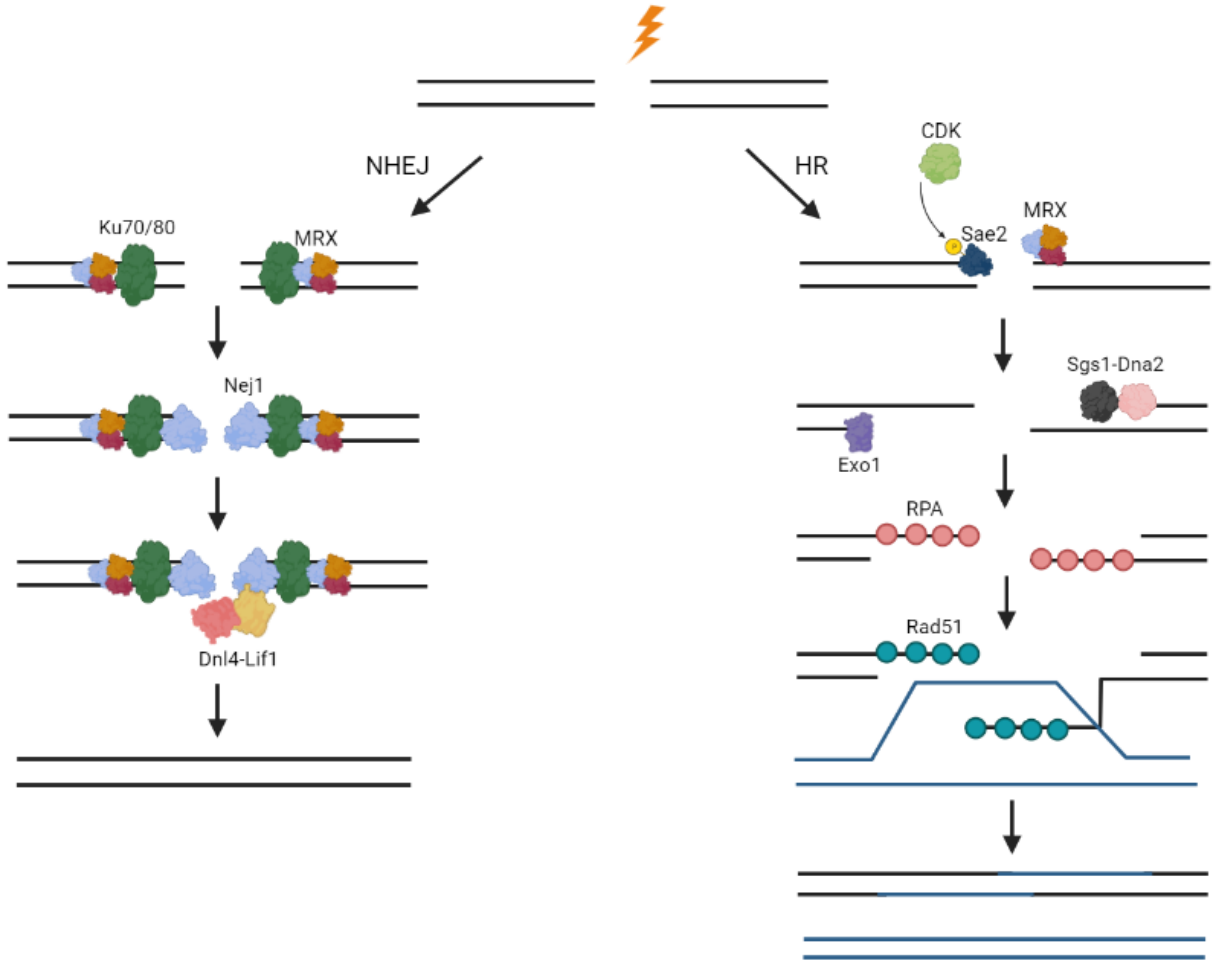

Figure 1.2 Repair of DNA DSBs by NHEJ and HR. When a DSB occurs in a cell, two main repair pathways exist in *S. cerevisiae* to repair the break: NHEJ and HR. If the more error-prone NHEJ pathway is chosen, simple re-ligation of the strands will fix the break. If the more precise HR pathway is chosen, processing of DNA ends occurs, and a homologous template (shown in blue) will be utilized to repair the break.

1.3 Rif1 and PP1 (Glc7)

1.3.1 Rif1

Rif1 is a conserved eukaryotic protein with diversified functions, originally identified as a telomere-binding protein in budding yeast (figure 1.3) (Mattarocci *et al*., 2016; Sreesankar *et al*., 2012). In *S. cerevisiae,* Rif1 negatively regulates telomere length by counteracting telomerase, an enzyme that extends telomeres (Zhong *et al*., 1992). This role, however, is not entirely conserved in human cells (Xu & Blackburn, 2004). Human Rif1 only binds aberrant telomeres, which are recognized as a site of DNA damage, and can signal a DNA damage response (DDR) (Xu & Blackburn 2004; Kumar & Cheok 2014). Mammalian and human Rif1 appear to be primarily involved with the organization of chromatin, regulation of the firing of origins of replication, and the DDR (Gnan *et al*., 2021; Alver *et al*., 2017; Buonomo *et al*., 2009).

The most recently discovered function of Rif1 appears to be its influence in DNA DSB repair pathway choice, whereby the literature suggests Rif1 acts to promote NHEJ. Yeast Rif1 has been shown to physically bind to DNA ends at DSBs to prevent DNA end degradation, and, thus, encourage repair by NHEJ (Mattarocci *et al*., 2017). Other studies have found that, in response to DNA damage by causes such as ultraviolet light, etoposide, and hydroxyurea (HU), a deoxyribonucleotide triphosphate pool reductor, human Rif1 interacts with other factors involved in the DDR, such as 53BP1, which promotes NHEJ (Kumar & Cheok 2014; Silverman *et al*.,

2004). Human Rif1 foci also colocalized with ataxia telangiectasia mutated (ATM) kinase, which functions as a signaling protein in DNA damage responses (Silverman *et al*., 2004; Zhou & Elledge, 2000). Furthermore, mouse Rif1 has been shown to interact with 53BP1 to promote NHEJ in early G1 and counteract BRCA1, a protein involved in HR which promotes end resection (Chapman *et al*., 2013; Prakash *et al*., 2015). Therefore, Rif1 appears to facilitate NHEJ, interacting with several factors involved in the DSB response.

Another function of Rif1 is in protecting nascent DNA from degradation at stalled forks during DNA replication. The replication process may come to a halt and stalling of replication forks may occur for a variety of reasons, such as DNA damage from inter-strand crosslinks, or drugs, like HU (Cortez, 2015). If ATM becomes activated due to the presence of stalled replication forks, it can phosphorylate SQ motifs of mouse Rif1, which has been shown to be essential in counteracting degradation of nascent DNA at stalled replication forks by the Dna2 nuclease (Balasubramanian *et al*., 2022). In a recent bioRxiv preprint, the removal of yeast Rif1 along with the removal of the Sgs1 helicase and Dna2 prevented nascent DNA degradation (Monerawela *et al*., 2020). These results suggest that the role of Rif1 at stalled replication forks operates in a way such that it regulates homologous recombination.

It, therefore, appears that Rif1 has a role in regulating which DSB repair pathway is chosen, seeming to promote NHEJ or counteract HR. While it is clear that Rif1 influences the DSB repair process, the exact mechanisms through which it does so remain elusive.

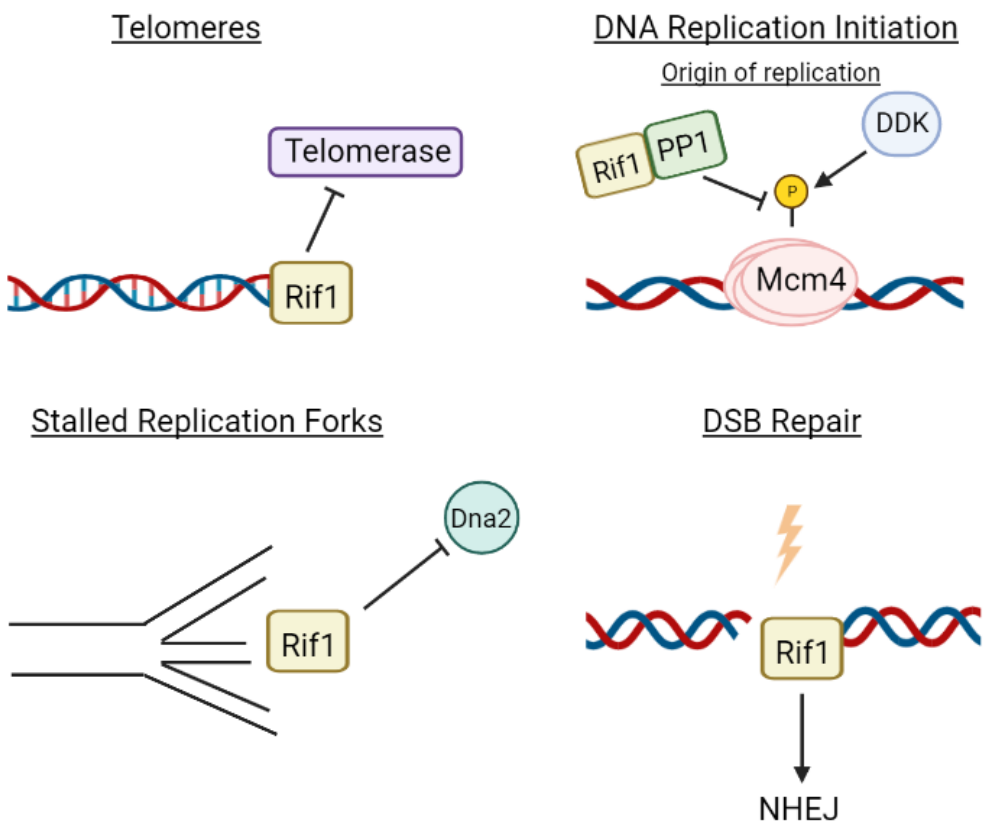

Figure 1.3. Roles of Budding Yeast Rif1. Yeast Rif1 is known for its diverse roles in telomere regulation, DNA replication initiation, stalled replication forks, and influencing DSB repair pathway choice. At telomeres, Rif1 functions to inhibit telomerase, an enzyme that extends telomeres. During DNA replication initiation, Rif1-PP1 maintain dephosphorylation of the Mcm2-7 helicase on Mcm4 to counteract DDK-mediated phosphorylation, thus preventing premature DNA replication. At stalled replication forks, Rif1 protects nascent DNA from degradation. Similarly, at DSBs Rif1 physically binds DNA ends to prevent resection by factors involved in HR, thereby promoting NHEJ.

1.3.2 PP1 (Glc7 in Budding Yeast)

Protein Phosphatase 1 (PP1) in mammalian cells, or Glc7 in budding yeast, is a vital enzyme in eukaryotes that takes part in an array of cellular processes, including apoptosis, cellular signaling, T-cell activation, DNA replication, and neuronal plasticity (Garcia *et al*., 2003; Aggen, *et al*., 2000; Shenolikar & Nairn, 1991). PP1 is a serine/threonine phosphatase that is involved with the majority of reversible dephosphorylation reactions (Bollen *et al.,* 2010). Phosphorylation events are one of the most frequently occurring post-translational modifications, influencing 30-70% of all proteins in eukaryotic cells, where PP1 alone forms complexes with approximately 650 mammalian proteins (Bollen *et al*., 2010). PP1 is a highly selective and regulated enzyme that has the ability to regulate the function of proteins, and conversely, be controlled by these same proteins. The catalytic subunit (PP1c) lacks intrinsic substrate specificity, but rather can form complexes with over 200 regulatory subunits to give PP1c target substrate specificity (Peti *et al*., 2013). The regulatory subunits target the catalytic subunit (PP1c) localizing PP1c near substrates to dephosphorylate specific phosphoserine or phosphothreonine residues in the substrate, or to decrease its dephosphorylation activity to other targeted substrates (Aggen *et al*., 2000).

While most regulatory subunits do not possess significant sequence similarities, they do share an RVxF motif in common, where PP1c can bind (Terrak *et al*., 2004). The RVxF motif is also seen in regulatory subunits in budding yeast, where Glc7, the PP1c homolog, can act as a substrate and interact with enzymes. However, there are mechanistic differences between

mammalian PP1 and yeast Glc7. A prime example of this is the catalytic subunit of PP1. Mammalian PP1 has 3 genes which encode for 4 different catalytic subunits of PP1: PP1α, PP1β/δ, PP1γ1 and PP1γ2 (Peti *et al*., 2013). Conversely, yeast Glc7p is the catalytic subunit of PP1 (Feng *et al*., 1991).

Glc7 was originally discovered for its role in regulating the phosphorylation state of glycogen synthase (Peng *et al*., 1990). It was later found to be a PP1 homolog, which came as no surprise, as PP1 was already a well-characterized regulator of glycogen metabolism (Cannon *et al*., 1994). Glc7 is not only involved in the regulation of glycogen, but also DNA replication, transcription, chromosome segregation, cell cycle progression and meiosis, to name just a few processes (Böhm & Buchberger, 2013; Tu & Carlson, 1995; Wu *et al*., 2001; Logan *et al*., 2008). While Glc7 has numerous PIPs, one of particular interest to our lab is its interaction with Rif1, due to its fundamental role in DNA replication timing and the DNA damage response.

1.3.3 Rif1-PP1

As mentioned above, Rif1 plays a critical role in the timing of DNA replication in both yeast and mammalian cells. First shown in 2014 by Mattarocci *et al*., this function of Rif1 is dependent on its interaction with PP1/Glc7. Specifically, Rif1 has two motifs where Glc7 docks, RVxF and SILK, which are conserved in eukaryotes (Mattarocci *et al*., 2014; Sreesankar *et al*., 2012). In the budding yeast, *Saccharomyces cerevisiae,* and the fission yeast,

Schizosaccharomyces pombe, these motifs are located in the N terminus. However, in *Homo sapiens*, these motifs are located in the C terminus of Rif1. These residues were found to be, in part, responsible for Glc7 binding at late-replicating telomeric regions, and likely at other Rif1-bound origins (Mattarocci *et al*., 2014; Kuntziger *et al*., 2006).

At replication origins in G1, Rif1 and Glc7 interact to prevent premature phosphorylation of the Mcm2-7 helicase, specifically ensuring Mcm4 remains dephosphorylated (Hiraga *et al*., 2014). Low levels of DDK activity in early G1 phase may be sufficient to prematurely phosphorylate the Mcm2-7 helicase, potentially resulting in early origin firing and, eventually, leading to genomic instability (Tanaka *et al*., 2011). Additionally, previous studies have demonstrated that the deletion of *RIF1* leads to an increase in premature phosphorylation of Mcm4 (Hiraga *et al*., 2014; Gnan *et al*., 2021). The interaction between Rif1 and Glc7 is, thus, crucial to maintain timely DNA replication and cell cycle regulation. While Rif1-Glc7 dephosphorylation activity in G1 is able to prevent Mcm helicase activity, DDK can conversely phosphorylate Rif1 in S phase near the RVxF motif, where Rif1 interacts with Glc7, disrupting their association (Kuntziger *et al*., 2006; Hiraga *et al*., 2014). The consequence of this is continuous phosphorylation of the Mcm helicase, thus, activating the CMG helicase, and allowing DNA replication to begin.

As indicated earlier, another role of Rif1 is in the DDR. Some of the observed phenotypes of Rif1 in relation to the DDR have been found to arise largely from its interaction with Glc7 (Mattarocci *et al*., 2014; Shyian *et al*., 2016; Hiraga *et al*., 2017). Yeast Rif1-Glc7 can prevent genomic instability by inhibiting rDNA origin firing (Shyian *et al*., 2016). This avoids an

accumulation of stalled replication forks, which can be detrimental to the cell as it may result in fork collapse and lead to an increase in DSBs, genome rearrangements, and cell death (Cortez, 2015; Zeman & Cimprich, 2014). In addition, human PP1 has been found to accumulate at DSBs through its interaction with Rif1 (Isobe *et al*., 2021). It appears that the ability of Rif1 and Glc7 to work together to influence the DDR is largely due to their role at replication forks during S phase and at DNA DSBs. However, further research is required to gain a deeper understanding of the underlying mechanisms responsible for the phenotypes observed in response to DNA damage, as this is yet to be well characterized.

1.3.4 Rif1 HOOK and Rif1 C466/C473

The most evolutionarily conserved region of Rif1 is its HOOK domain (Finn *et al*., 2016; Fontana *et al*., 2018). The crystal structure of Rif1 exhibits a head-to-tail dimer that forms a figure 8 conformation with two DNA binding channels in the spaces between each head and tail (Fontana *et al*., 2018). These channels, I and II, are capable of threading through two separate DNA molecules (figure 1.4B). A DNA strand will thread through channel I on one Rif1 dimer, and then channel II of another Rif1 dimer, which connects neighboring dimers (Mattarocci *et al*., 2017). Rif1 binds nonspecifically to the negatively charged DNA via its positively charged residues residing in the HOOK domain (Mattarocci *et al*., 2017).

In *S. cerevisiae,* five specific Rif1 amino acid residues have recently been found to be crucial for Rif1's role at DNA DSBs (figure 1.4A) (Mattarocci *et al*., 2017; Fontana *et al*., 2019). Three of these are lysine residues, K437, K563 and K570, residing in the HOOK domain of

Rif1's N terminal region and the other two are cysteine residues, C466 and C473, similarly residing in the N terminus. These five residues have been demonstrated to be essential for Rif1 to promote NHEJ in response to DSBs (Mattarocci *et al*., 2017; Fontana *et al*., 2019).

The three lysine residues that were characterized by Mattarocci *et al*., 2017 were discovered as a consequence of a search for potential residues responsible for Rif1's DNA-binding abilities. Twelve positively charged residues were discovered on the concave face of the HOOK domain where DNA is bound closest. Of these twelve residues, K437, K563, and K570, were mutated to glutamic acid and the resultant mutant protein could be stably expressed. Through this mutant Rif1, named $Rif1_{HOOK}$, the authors were able to demonstrate that these residues are essential in order for Rif1 to counteract DNA end resection by binding DNA at telomeres and DSBs. In a reporter strain, whereby a DSB can be induced by HO endonuclease at the MAT locus and can only be repaired by NHEJ, the $Rif1_{HOOK}$ strain resulted in a 40% decrease in cell survival compared to *RIF1* WT cells, phenocopying *rif1*Δ cells. $Rif1_{HOOK}$ was also found to result in increased ssDNA accumulation at the MAT locus after an HO endonuclease-induced DSB compared to WT *RIF1*. These results suggest the lysine residues in the HOOK domain of Rif1, K437, K563 and K570, are important for modulating NHEJ at DSBs (Mattarocci *et al*., 2017).

Additionally, the two cysteine residues in Rif1, C466 and C473, play a significant role in Rif1's effect at DSBs. These residues were found by Fontana *et al*. in 2019 to influence DSB repair by the palmitoylation of residues, C466 and C473, by the palmitoyltransferase, Pfa4, allowing Rif1 to localize to the inner nuclear membrane. They found that S-palmitoylation of

these two Rif1 cysteine residues prevents DNA end-resection at DSBs and are required to promote repair by NHEJ. Rif_{NTD} (residues 1–1322 of Rif1) was shown to localize to the inner nuclear membrane independently of cell cycle phase in response to the treatment of Zeocin, a DSB-inducing agent, or ionizing radiation (IR), but dependent on Pfa4, S-acylated residues C466 and C473, or the HOOK domain. A Rif1 strain with the combined mutations C466A/C473A and K437E/K563E/K570E, thereby disrupting Rif1's activity in localizing to the inner nuclear membrane and binding DNA, resulted in even less formation of Rif1 foci upon zeocin exposure than these two sets of mutations on their own (Fontana *et al*., 2019). Therefore, both these sets of cysteine and lysine residues are important for Rif1-mediated NHEJ promotion to repair DSBs.

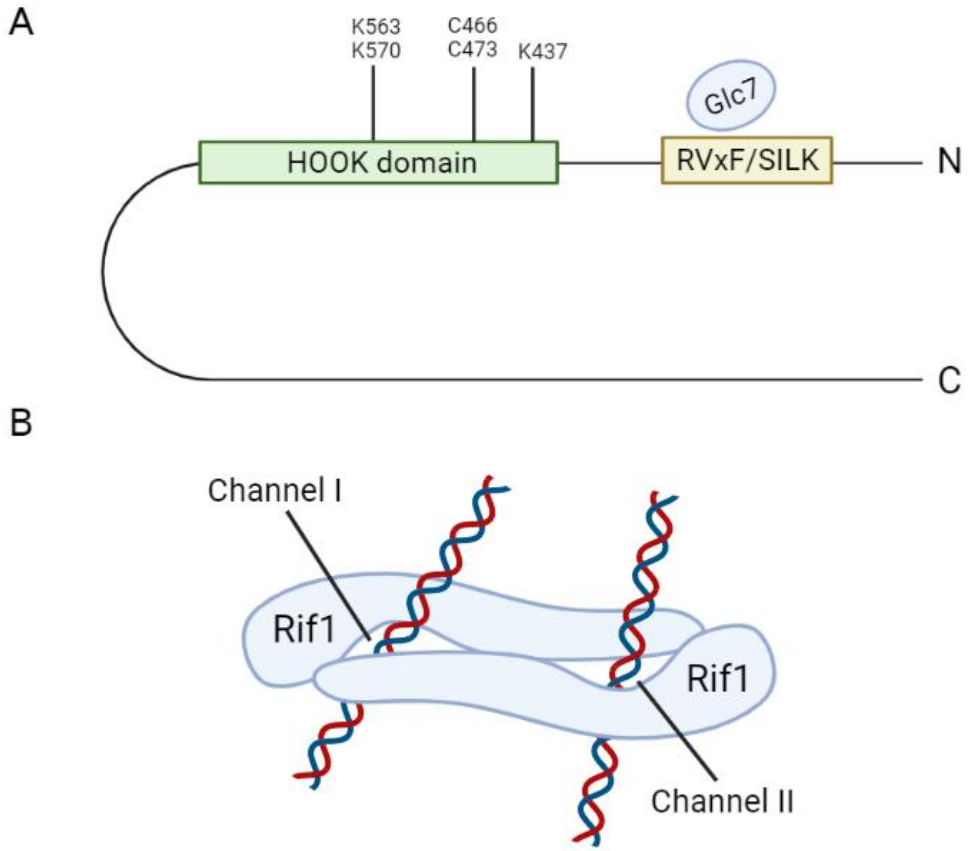

Figure 1.4. Map and structure of yeast Rif1. (**A**) Schematic representation of budding yeast Rif1 in a horseshoe conformation. The HOOK domain, encompassing part of the N terminus, is highlighted in green and contains the lysine residues, K437, K563, and K570, and the cysteine residues, C466 and C473. The RVxF/SILK motif where Glc7 binds is shown in yellow. (**B**) A Rif1-dimer in a head-to-tail conformation threading two DNA strands through channel I and II.

1.4 Research Objectives

There is clear evidence suggesting a novel function for Rif1-Glc7 at DNA DSBs. Based on the literature and previous findings in the Duncker lab, the hypothesis at the outset of my thesis research was that constitutive interaction between Rif1 and Glc7 influences the DSB repair process by strongly promoting the error prone NHEJ pathway, thus resulting in hypersensitivity to reagents that provoke the formation of DSBs.

Evidence that Rif1 interacts with and directs PP1/Glc7 to various proteins in DNA replication initiation and during DNA DSB repair continues to emerge (Hiraga *et al*., 2017; Isobe *et al*., 2021; Garzón *et al*., 2019). My research objectives aimed to confirm that the S-palmitoylation and HOOK domain residues, C466A/C473A and K437E/K563E/K570E, respectively, of Rif1 contribute to its role in repair pathway choice. Furthermore, a key objective was to examine whether these mutations rescue DSB hypersensitivity in a strain where Rif1 and Glc7 can constitutively interact and have shown to be hypersensitive to the DSB-inducing agents, bleocin and phleomycin. I also aimed to assess the cause of hypersensitivity in this constitutively active Rif1-Glc7 strain was related to changes in DSB resection.

My specific goals sought to investigate the following in *Saccharomyces cerevisiae*.

1. Confirm that abrogating the interaction between Rif1 and Glc7, through its RVxF/SILK motif, in a strain where Rif1-Glc7 activity is upregulated and shown to be sensitive upon exposure of DSB-inducing agents, results in rescue of hypersensitivity via a decrease in NHEJ.

2. Create C466A/C473A and K437E/K563E/K570E mutations in both wild type cells and a strain with constitutive Rif1-Glc7 activity to assess the requirement of Rif1's presence at and physical binding to DNA in rendering cells hypersensitive to DSBs.
3. Assess whether preventing Rif1 from localizing to DSBs, through addition of C466A and C473A mutations, to the strain indicated in goal 1, further rescues hypersensitivity beyond simply abrogating Rif1's interaction with Glc7 through the RVxF/SILK motif.
4. Determine relative resection at DNA DSBs in a strain where Rif1-Glc7 activity is upregulated, compared to wild type *RIF1*.

1.5 Research Significance

Cancer is the second-leading global cause of death and takes 10 million lives every year (Matos *et al*., 2021; Sung *et al*., 2021). While female breast cancer represents the highest number of cancer diagnoses per year, lung cancer is responsible for the majority of cancer deaths (Sung *et al*., 2021). The search for new drug therapies by targeting endogenous proteins and genes has been ongoing, with the first targeted cancer therapy approved in the 1970s (Cole *et al*., 1971; Yan *et al*., 2011). In recent years, both Rif1 and PP1 are being recognized for their potential as drug targets in cancer treatment.

Rif1 has been shown to be upregulated in a variety of cancers, including breast and cervical cancer, and more recently, non-small cell lung carcinoma (NSCLC) (Mei *et al*., 2017;

Mei *et al*., 2018b). Interestingly, in NSCLC, Rif1 has been shown to promote NHEJ, and likely does this by targeting a known oncogene, MYC (Mei *et al*., 2018b), which may suggest an alternative method of how Rif1 modulates NHEJ in addition to the ones mentioned in this thesis. There is a positive correlation between Rif1 expression and the expression of MYC activating genes, such as PARP1 and LIG4, which are both involved in the repair of DSBs by NHEJ (Mei *et al*., 2018b; Caron *et al*., 2019). Knockdown of Rif1 in NSCLC cells resulted in the downregulation of downstream MYC targets, and in mice tumor tissues, the knockdown of Rif1 blocked MYC expression and inhibited tumor growth (Mei *et al*., 2018b).

Interestingly, the targeting of PP1 by Rif1 to dephosphorylate AXIN, and thereby activate Wnt/β-catenin signaling in NSCLC, results in tumor growth and cancer stem cell (CSC)-like properties (Mei *et al*., 2018a). Growth and CSC-like traits were counteracted by inhibiting PP1 in Rif1-overexpressed cells, along with the downregulation of the Wnt/β-catenin signaling (Mei *et al*., 2018a). In contrast to these results, another study showed that adenocarcinoma patients with low levels of the PP1 catalytic subunit genes, PPP1CA/B, had a significantly increased risk of lower survival rates than patients who had high expression levels of these two genes (Verdugo-Sivianes *et al*., 2017). Thus far, the literature suggests that the expression level of PP1 in functioning as a tumor promoter or suppressor is dependent on the type of cancer.

There is clear evidence for a role of Rif1-PP1 in tumorigenesis and cancer, yet the mechanisms through which this occurs remain to be uncovered. While the research conducted in this thesis uses the model organism *Saccharomyces cerevisiae*, these experiments will

nonetheless contribute to the understanding and current knowledge on the mechanisms of Rif1-PP1 in DNA DSB repair and its potential as an anti-cancer drug target.

Chapter 2

Materials & Methods

2.1 Yeast Strains

The yeast strains displayed in the following table were used in the experiments of this thesis. All yeast strains generated in this study were created using CRISPR-Cas9.

Table 2.1. Yeast Strains in this Study.

Strain	Genotype	Source
BY4741	*MATa, his3Δ1, leu2Δ0, met15Δ0, ura3Δ0*	Brachmann *et al*., 1998
DY-361	*MATa, his3Δ1, leu2Δ0, met15Δ0, ura3Δ0, RIF1 MYC::HIS3MX6*	Larasati, 2020
DY-364	*MATa, his3Δ1, leu2Δ0, met15Δ0, ura3Δ0, Δmre11::URA3*	Larasati, 2020
DY-380	*MATa, his3Δ1, leu2Δ0, met15Δ0, ura3Δ0, rif1 5AΔPPDSPP MYC::HIS3MX6*	Larasati, 2020
DY-392	*MATa, his3Δ1, leu2Δ0, met15Δ0, ura3Δ0, rif1 RVxF/SILK MYC::HIS3MX6*	Larasati, 2020
DY-393	*MATa, his3Δ1, leu2Δ0, met15Δ0, ura3Δ0, rif1 RVxF/SILK-5AΔPPDSPP MYC::HIS3MX6*	Larasati, 2020
DY-418	*MATa his3Δ1, leu2D0, met15D0, ura3D0 RIF1 MYC::HIS3MX6, leu2::*P_{lexO}*-AscI-*T_{CYC1}*-*P_{ACT1}*-LexA-ER-B112-*T_{CYC1}*-LEU2MX*	This study
DY-419	*MATa his3Δ1, leu2D0, met15D0, ura3D0 rif1 5AΔPPDSPP MYC::HIS3MX6, leu2::*P_{lexO}*-AscI-*T_{CYC1}*-*P_{ACT1}*-LexA-ER-B112-*T_{CYC1}*-LEU2MX*	This study
DY-429	*MATa, his3Δ1, leu2Δ0, met15Δ0, ura3Δ0, rif1-K437E-K563E-K570E MYC::HIS3MX6*	This study
DY-430	*MATa, his3Δ1, leu2Δ0, met15Δ0, ura3Δ0, rif1 5AΔPPDSPP-K437E-K563E-K570E MYC::HIS3MX6*	This study
DY-431	*MATa, his3Δ1, leu2Δ0, met15Δ0, ura3Δ0, rif1-C466A-C473A MYC::HIS3MX6*	This study
DY-432	*MATa, his3Δ1, leu2Δ0, met15Δ0, ura3Δ0, rif1 5AΔPPDSPP-C466A-C473A MYC::HIS3MX6*	This study

DY-433	*MATa, his3Δ1, leu2Δ0, met15Δ0, ura3Δ0, rif1 RVxF/SILK-5AΔPPDSPP-C466A-C473A MYC::HIS3MX6*	This study

2.2 Plasmid Construction

The plasmids displayed in the following table were used in the experiments of this thesis. The PML104 plasmid was modified to contain DNA sequence specifying a single-guide RNA (sgRNA) targeting a region of DNA within the Rif1 gene of *S. cerevisiae*. For example, "PML104 + Rif1 C466 sgRNA" is the PML104 plasmid with ligated dsDNA encoding the sgRNA that will target the region of Rif1 encoding C466.

Table 2.2. Plasmids in this Study.

Plasmid	**Source**
PML104	Laughery *et al*., 2015
PML104 + Rif1 C466 sgRNA	This study
PML104 + Rif1 C473 sgRNA	This study
PML104 + Rif1 K437 sgRNA	This study
PML104 + Rif1 K563/K570 sgRNA	This study
pRG645_lexO-AscI_LexA-TF_LEU2MX	Gnügge & Symington, 2020
pCM190-myc13	(Larasati, 2020)

pCM Rif1 Myc	(Larasati, 2020)

The PML104 plasmids used in this study were adapted to contain DNA sequences that each encoded a sgRNA designed using Benchling's CRISPR function and a previous study (https://benchling.com; Laughery et al., 2015). Specifically, the gRNA component of the sgRNA was designed using Benchling, and the 5' overhang and 5' end of the structural segment were obtained from Laughery *et al*., 2015. The design type selected on Benchling was "single guide" and the guide length was set to 20 nucleotides (nts). The Rif1 gene sequence was uploaded, and a list of potential DNA sequences that encode gRNAs was provided for our target region. The gRNA was chosen based on the on- and off-target scores, where the on-target score represents the cleavage efficiency of Cas9, and the off-target score represents the probability of Cas9 binding to off-target sites. A 'GATC' overhang was added to the 5' end of the top strand of the DNA sequence that encodes the gRNA, since this sequence will be ligated into a plasmid, PML104, that was digested with the BclI restriction enzyme, which leaves a 'CTAG' overhang and SwaI, which results in a blunt end. Additionally, PML104 contains the 3' end of the sgRNA, which contains the SwaI cut site. Therefore, a 5' structural component was added to the gRNA to complete the sgRNA (5'-GTTTTAGAGCTAG-3'). The sgRNA, therefore, contains the 5' 'GATC' overhang on the top strand, the gRNA, and the 5' structural component (Laughery *et al*., 2015). The DNA encoding the sgRNA was produced via Eurofins Genomics (https://eurofinsgenomics.com).

DAM- S255 *E. coli* cells, which contain the PML104 plasmid (addgene #67638) conferring resistance to ampicillin, were grown overnight at 37°C on LB and 100 µg/ml ampicillin (Laughery *et al*., 2015). Plasmid extraction was carried out with a miniprep kit (Geneaid #PDH300), and the plasmid was digested with the restriction enzymes, BclI and SwaI. To allow for directional cloning, SwaI, which results in a blunt end, and BclI, which results in a sticky end, were used. The annealed dsDNA encoding the sgRNA can ligate to the digested vector using the BclI sticky end. The top and bottom DNA strand encoding the sgRNA were annealed using T4 ligase, which joins the DNA together, and a thermal cycler (95°C for 6 minutes, -1°C/minute until reaction reaches 25°C). Annealing was confirmed by running a 2% agarose gel at 100V for 1 hour, which allowed for the visualization of the annealed DNA encoding the sgRNA by a band of approximately 30-40bp (ChemiDoc MP; BioRad).

The DNA encoding the sgRNA insert was added to the vector in a molar ratio of 6:1, respectively, and ligation was done using a T4 DNA ligase kit (BioBasic). To confirm ligation, a 0.6% agarose gel was run at 100V for 1 hour, which allowed for the visualization of the digested vector and re-ligated vector. Gels were imaged using the BioRad ChemiDoc MP imager. The ligated vector, containing the dsDNA encoding for the sgRNA, denoted as "PML104 + sgRNA", was transformed into $CaCl_2$ competent DH5α *E. coli* cells. These cells were plated on LB containing 100 µg/ml ampicillin and left to grow overnight at 37°C. Colonies were selected in LB liquid media containing 100 µg/ml ampicillin and grown overnight at 37°C. The vector was isolated using a miniprep kit (Geneaid #PDH300). To confirm the dsDNA encoding the sgRNA had ligated to the vector, the plasmid samples were sent to SickKids TCAG Facilities in Toronto

for sequencing (SickKids, Toronto, Ontario, Canada). Plasmid samples were sent using the SickKids TCAG guidelines of 300 ng of plasmid in a total volume of 7 µl.

The pCM Rif1 Myc plasmid was constructed from a pCM190-myc13 vector by Larasati. Full length Rif1 was amplified from BY4741, digested with BamH1 and Not1, and cloned into a pCM190-myc13 vector with gel extraction and cloning (Larasati, 2020).

2.3 List of Primers

The primers displayed in the following table were used in the experiments of this thesis for polymerase chain reaction (PCR), sequencing or quantitative PCR (qPCR), as indicated in table 2.3. When samples were sent for sequencing to SickKids TCAG Facilities, 0.7 µl of 5 µM forward or reverse primer was added to 50 ng of cleaned PCR product in a total volume of 7 µl, as per their guidelines. PCR products were cleaned using a kit (Geneaid #DFC300).

Table 2.3. List of Primers Used in this Study.

Primer	Forward primer	Reverse primer	Source
DSB primers at chromosome 7 (for qPCR)	5'-ACATGTAATTGGCAC AGGGA-3'	5'- GGGCGTCGTTATTG CAAACT -3'	This thesis

Primer 3 and 4 (CTRL primers for qPCR)	Primer 3: 5’-CCCACAAGTCCTCTG ATTTACATTCG-3’	Primer 4: 5’-ATTCGATTGACAGGT GCTCCCTTTTC-3’	Ferrari *et al*., 2018
1kb Rif1 primer (for PCR and Sequencing)	5’-TCATAACAGCACAA GTCTC-3’	5’- GGTCCCAAAATAGT TCAAAC -3’	This thesis
pRG205MX p3 and p1	p3: 5’- ACCGTTAAGTCTCA AGCAAAGG-3’	p1: 5’- CTGTGTGAAATTGT TATCCGCTCAC-3’	Gnügge *et al*., 2016
pRG205MX p2 and p5	p2: 5’-GGTTAGCCTGCGGA TCATATG-3’	p5: 5’- GTTCAAGAAGGTAT TGACTTAAACTCCATC-3’	Gnügge *et al*., 2016

2.4 CRISPR-Cas9

CRISPR-Cas9 was used to introduce point mutations into the *RIF1* gene in the model organism, *S. cerevisiae*. This method requires design of a sgRNA for the top and bottom strand,

which was completed using Benchling and the protocol described in Laughery *et al*., 2015, as detailed previously in section 2.2, and design of a single-stranded (ss) repair cassette. Once the DNA encoding the sgRNA had been successfully inserted into the PML104 plasmid, which also contains the gene for the Cas9 endonuclease, the strains underwent lithium acetate yeast transformation, as described in section 2.4.1. When the plasmid is taken up into yeast cells via lithium acetate yeast transformation, both the Cas9 endonuclease and the sgRNA will be expressed and will join to form a ribonucleoprotein complex. Since the sgRNA has homology to the site where the mutation will be made in the *RIF1* gene, it directs Cas9 there, where Cas9 can then induce a DSB.

The ss repair cassette requires a minimum of 40 nts of homology to the *RIF1* gene on either side of the portion of the DNA that contains the mutation and protospacer adjacent motif (PAM). The PAM sequence is an adjacent motif that Cas9 will recognize and cleave 3-4 nts upstream of. When making the repair cassette, the region encoding the PAM sequence, 'NGG', where N is any nucleotide preceding two guanines, must be altered, while maintaining the same amino acids, to prevent subsequent cutting of the repair cassette by Cas9. Since the repair cassette contains a region of homology on either side of the altered section in the cassette, the cell should use homology-directed recombination to repair the DSB that Cas9 creates, and the mutation, along with the altered PAM sequence, should be incorporated into the gene. Once the repair cassette was designed, the oligo was produced by Eurofins Genomics (https://eurofinsgenomics.com).

The sgRNAs and ss repair cassettes displayed in the following table were used in the experiments of this thesis. The gRNA component of all sgRNAs were designed using Benchling and repair cassettes were designed by myself.

Table 2.4. List of sgRNAs and Repair Cassettes.

Mutation	**sgRNA Top Strand**	**sgRNA Bottom Strand**	**ss Repair Cassette**
K437E	5’-GATCTACCAGGTGAGGTACTACCTGTTTTAGAGCTAG -3’	5’-CTAGCTCTAAAACAGGTAGTACCTCACCTGGTA-3’	5’-TGAGACGGTAACTTCTTGGTTACCAGGTGAGGTACTACCTAGAATTATTATCGGAGATGAAATTTACTCCATGGAAATTCTCATAACTTCAATAGTTGTTTTACTGGAACTACTAA-3’
K563E/ K570E	5’-GATCGATGGACATTAAGCGAGTCTGTTTTAGAGCTAG -3’	5’-CTAGCTCTAAAACAGACTCGCTTAATGTCCATC-3’	Top: 5’-TGGTTTGATTTAAATAACCTGTGCTTTATCAATAATCACCCCAAGACTCGCTTAATGTCCATCAAAGTTTGGAG

			AATTATTACCTACTGCATA TGCACGAAAATAT-3’ Bottom: 5’- ATATTTTCGTGCATATG CAGTAGGTAATAATTCTCC AAACTTCGATGGACATTA AGCGAGTTTCTGGGTGATT ATTGATAAAGCACAGGTT ATTTAAATCAAACCA-3’
C466A	5’-GATCCTGGA GATAGCATGAT ACACGTTTTAG AGCTAGC-3’	5’-GCTAGCTCTA AAACGTGTATCA TGCTATCTCCAG- 3’	5’-AAAAATGCTTAGATTTT GTTGATGAACATGAAAGG ATTTATCAGGCTATCATGC TATCTCCAGTATGCGAAAC AATCCCGGAAAAAT-3’
C473A	5’-GATCTCCAG TATGCGAAACA ATCCGTTTTAG AGCTAG-3’	5’-CTAGCTCTAA AACGGATTGTTT CGCATACTGGA- 3’	Top: 5’-ACATGAAAGGATTTAT CAGGCTATCATGCTATCTC CAGTAGCCGAAACAATCC CAGAAAAATTTTTATCTAA

	ACTACCGTTAAATTCATAT GACAG-3’ Bottom: 5’-CTGTCATATGAATTTAA CGGTAGTTTAGATAAAAA TTTTTCTGGGATTGTTTCG GCTACTGGAGATAGCATG ATAGCCTGATAAATCCTT TCATGT-3’

As an optimization measure of CRISPR-Cas9, both the top and bottom ss repair cassettes were added during yeast transformation for the C473A and K563E/K570E mutations, as opposed to only the top strand, which was the case for the other mutations. By adding both the top and bottom strand of the ss repair cassette during yeast transformation, we were able to increase the efficiency of transforming the cassette and, thus, successfully create the desired mutation at a faster rate.

2.4.1 Yeast Transformation

After the PML104 plasmids were constructed to encode their respective sgRNAs, lithium acetate yeast transformation was carried out to incorporate the PML104 + sgRNAs and repair cassettes into the yeast strains DY-361 and DY-380, at a ratio of 5 µg of repair cassette to 400 ng of plasmid + sgRNA. Similarly, DY-393 was transformed with the C466A and C473A PML104 + sgRNAs and respective ss repair cassettes.

The yeast strains prior to transformation were grown to a working concentration of ~$1x10^7$ cells/ml in 10 ml of YPD (10% yeast extract, 20% peptone, 20% dextrose). These cultures were centrifuged at 4000 rpm for 5 minutes, the supernatant was decanted, and the pellet was resuspended in 10 ml of 1 X Tris-EDTA (TE), pH 8.0. This resuspension was centrifuged again at 4000 rpm for 5 minutes, the supernatant was decanted, and the pellet was gently resuspended in 2 ml of lithium acetate (LiAc)/TE solution (100 mM lithium acetate, 0.5x TE) and incubated for 10 minutes at room temperature (RT). In a 1.5 ml microcentrifuge tube, the following contents were added in order: PML104 + sgRNA, 100 µg of ss salmon sperm DNA (already boiled for 10 minutes at 100°C and iced until cool), 100 µL of yeast suspension, repair cassette, 300 µL of LiAc/TE/PEG4000 mix (100 mM lithium acetate, 40% PEG4000, 1 X TE) gently mixed with a P1000. Negative controls were used for each strain and contained everything as previously stated, except the PML104 + sgRNAs and ss repair cassettes. The tubes were incubated for 30 minutes at 30°C. Next, 40 µL of dimethylsulfoxide (DMSO) was added, and the yeast suspension was gently mixed with a P1000 pipette. Cells were heat shocked for 7 minutes at 42°C and immediately iced for 2 minutes. Cells were plated on synthetic complete (SC) media

without uracil, because the PML104 plasmid contains a URA3 selectable marker. After 2-3 days of the yeast transformants growing at 30°C, 4-5 colonies from each yeast transformation plate were selected and inoculated in 10 ml YPD, as the plasmid is no longer needed and, thus, double selection is not necessary, and left shaking at 250 rpm at 30°C until yeast cultures reached saturation (~24-48 hours). Frozen permanent stocks were made by adding 500 µl of yeast saturated culture of the transformant and 500 µl of 60% glycerol to a 2 ml screw cap tube and freezing in liquid nitrogen. Frozen permanents were stored at -80°C.

2.4.2 Plasmid Curing

Since strains for which C466A/C473A and HOOK mutations were being generated had to undergo two rounds of CRISPR-Cas9 mediated modification, the first PML104 construct had to be removed in order to allow transformation of the second PML104 construct and selection again on SC-ura medium for the second set of mutations. This was achieved by plating the yeast strains with the first successful mutation on SC plates containing 0.25 g 5'-Fluoroorotic acid (5FOA) in 250 ml SC media, which is toxic to yeast cells with a URA3 gene. 5FOA converts uracil into 5-fluorouracil, which consequently leads to cell death (Møldrup *et al*., 2012). After cells were plated on 5FOA, 2-3 colonies were selected and grown in 10 ml YPD liquid media overnight at 30°C, shaking at 250 rpm. These cells were then plated on YPD and SC-ura solid media to confirm the loss of the plasmid. The strains that did not grow on SC-ura and grew on YPD, suggesting loss of plasmid, were selected, and grown in 10 ml YPD liquid media overnight at 30°C shaking at 250 rpm. Frozen permanents were created of these saturated cultures, as

described above, and stored at -80°C. A strain containing the PML104 plasmid was used as a control, in which growth on both YPD and SC-ura was expected.

2.5 Genomic DNA Extraction and Analysis

Yeast colonies selected for analysis were grown in 10 ml YPD at 30°C overnight shaking at 250 rpm, and frozen permanents were made, as described previously. The rest of the yeast culture was centrifuged at 4000 rpm for 5 minutes, followed by removal of the supernatant, resuspension of the pellet in 500 µL of sterile Milli-Q water, and transferred to a 2 ml screw cap tube for genomic DNA extraction. This resuspension was microcentrifuged at 4000 rpm for 10 seconds, the supernatant was removed, and the pellet was loosened by vortex at a low speed. The loose pellet had 200 µL of genomic prep mix (2% Triton X-100, 1% SDS, 100 mM NaCl, 10 Mm Tris-Cl (pH 8), 1 mM EDTA) added, 200 µL of phenol:chloroform:isoamylalcohol (25:24:1, v/v) and approximately 0.5 g of 0.5 mm glass beads. The mixture was vortexed for 3-4 minutes at maximum speed. Next, 200 µL of 1 X TE (pH 8) was added to the mixture, which was then vortexed briefly, and centrifuged for 5 minutes at 4000 rpm. The supernatant was transferred to a new 1.5 ml microcentrifuge tube, along with 1 ml of 100% ethanol, and the rest of the mixture was discarded. The tube containing the supernatant and ethanol was inverted to mix and centrifuged for 2 minutes at 4000 rpm. After centrifugation, the supernatant was decanted, and the pellet was resuspended in 400 µL 1 X TE (pH 8). Next, 10 µL of RNase A at a concentration of 10 mg/ml was added to the tube, and then incubated at 30°C for 10 minutes. Following this, 10 µL of ammonium acetate (4 M) and 1 ml of 100% ethanol were added and

inverted to mix. The tube was then centrifuged for 2 minutes at 4000rpm, the supernatant was decanted, and the pellet was left to air dry for approximately 20 minutes, before the pellet was resuspended in 50 µL of 1 X TE (pH 8). The concentration of the genomic DNA was determined using a NanoDrop 2000 (ThermoFisher). Genomic DNA preps were stored at -20°C.

PCR was used to amplify the region where the point mutation(s) were made, which could be sent to SickKids TCAG Facility to confirm the desired mutations were present. Primers were designed to encompass an ~800-1000 bp region, in which the middle included the mutation site. The primers were designed by myself based on 3 general guidelines: length of primers are 18-22 bp, GC content is 30-80%, and the primers in a pair have a Tm within 5°C of each other and are between 65°C-75°C, as recommended by ThermoFisher (https://www.thermofisher.com/blog/behindthebench/pcr-primer-design-tips/). PCR was carried out using a commercially available 2x GB-AMP™ PaCeR™ HP™ Master Mix (GeneBio Systems), along with 100 ng of genomic DNA, and 10 µM each of forward and reverse primers (table 2.3). A T100 thermal cycler (Bio-Rad) was used with the following program:

1. 95°C for 3 minutes
2. 95°C for 15 seconds
3. 55-65°C for 15 seconds
4. 72°C for 15-30 sec/ kb
5. 30X repeat of steps 2 to 4
6. 72°C for 5 minutes

All PCR products were run on a 2% agarose gel at 100V for 1 hour and visualized using a Bio-Rad ChemiDoc MP imager and SafeView DNA staining (abm #G108). PCR products were cleaned using a PCR clean up kit after gel analysis (Geneaid #DFC300). Steps 3 and 4 vary depending on melting temperature of primers used and length of amplicon, respectively.

2.6 Spot Plate Assay

Yeast strains were grown in 10 ml YPD for 48 hours at 30°C until they reached saturation. Cultures were serially diluted 10-fold 5 times on YPD medium or YPD medium containing a genotoxic agent, zeocin (ThermoFisher #R25001) or phleomycin (Sigma Aldrich #P9564), which were added to YPD media while pouring plates Plates were incubated at 30°C and imaged after 48 hours using an imager (ChemiDoc MP; Bio-Rad).

2.7 Resection Assay

2.7.1 Modification of Yeast Strains for Inducible DSB Generation

To modify yeast strains so that DSBs could be induced, the *lexO-AscI* system was utilized (Gnügge & Symington, 2020). This system involves an integrative plasmid, pRG645 LexO-AscI LexA-TF LEU2MX (pRG645), developed from the pRG205MX plasmid (Gnügge *et al.*, 2016). These plasmids were designed to integrate into auxotrophic yeast strains, including the designer deletion auxotrophic strains, specifically at the region of the deleted *LEU2* gene

(Brachmann *et al*., 1998). The pRG645 plasmid is comprised of an engineered transcription factor, LexA-ER-B112, an AscI restriction enzyme under the P_{lexO} promoter, a *LEU2MX* gene, and two AscI restriction enzyme cut sites, which encompass a region containing a bacterial selection marker *bla* (β-lactamase), and a bacterial origin of replication.

Firstly, the pRG645 plasmid, obtained from addgene (#154813), was isolated using a miniprep kit (Geneaid #PDH300) and linearized via a digest with AscI for 15 minutes at 37°C (FD#1894, ThermoFisher). Digestion was confirmed using a 0.6% agarose gel at 100V for 1 hour, in which bands 8076bp and 2083bp were visualized using a BioRad ChemiDoc MP imager and SafeView DNA staining (abm #G108). The integrative portion is the larger fragment and contains homology to the designer deletion strains where the *LEU2* gene was deleted. Lithium acetate yeast transformation was carried out, as described previously in section 2.4.1, with the digested plasmid and plated on selective media lacking leucine (SC -leu). Yeast transformants were selected and grown in 10 ml of liquid YPD media overnight at 30°C, shaking at 250 rpm. To ensure the plasmid had properly integrated, 500 µl of saturated culture was stored as a glycerol stock at -80°C, as described previously in section 2.4.1, and the rest of the culture underwent genomic DNA extraction, PCR using primers pRG205MX p1, p2, p3, and p5, and run on a 2% agarose gel at 100V for 1 hour. Bands were visualized using SafeView DNA staining (abm #G108) and an imager (ChemiDoc MP; BioRad). Primers pRG205MX p3 and p5 are complementary to the plasmid DNA and pRG205MX p1 and p2 are complementary to the yeast genome (table 2.3). Primer p3 is a forward primer and p1 is the reverse primer encompassing a 272 bp region, whereas p2 is a forward primer and p5 is the reverse primer, encompassing a 365

bp region. Both sets of primers were used to confirm integration of the pRG645 plasmid at the desired locus. Integration was completed in both *WT Rif1* (DY-361) and *rif1 5A*Δ*PPDSPP* (DY-380).

2.7.2 qPCR for Resection Assay

Cells from DY-361and DY-380 containing the integrative pRG645 plasmid were grown overnight at 30°C, shaking at 250 rpm in 25 mL YPD media to reach a concentration of ~$5x10^5$ cells/ml. A 6 mL sample was collected and pelleted by centrifugation at 5000 rpm for 5 minutes at time 0, before induction began, and kept on ice. To the rest of the cells, 2 µM of β-estradiol was added and cells were kept at 30°C, shaking at 250 rpm. Samples of 6 mL were collected every 2 hours until 6 hours was reached. Upon collection of samples, 0.1% sodium azide was added to cells to freeze cell metabolism, and cells were stored on ice. At the end of collection, samples t=2, t=4 and t=6 were pelleted and all time-points were stored on ice at 4°C. The next day, genomic extraction was carried out following the genomic DNA extraction protocol described previously in section 2.5. After genomic DNA was extracted and concentration was determined via the nanodrop, samples were either digested or mock-digested using 2.5 µg of genomic DNA with the restriction enzyme, Hpy188iii (NEB #R0622), and 10X rCutSmart Buffer (NEB) at 37°C for 1 hour. Mock-digested samples consisted of the same components as the digested samples with the exception of the restriction enzyme. Afterwards, the samples were incubated at 65°C for 20 minutes to heat inactivate the enzyme. The DNA was precipitated with an equal part of isopropanol and centrifuged at max speed for 30 minutes. The supernatant was

carefully removed, and 1 mL of cold 70% ethanol was added. Samples were centrifuged for 5 minutes at max speed and carefully decanted. Pellets were left to air dry and resuspended in 100 µl 1x TE (protocol adapted from Ferrari *et al.*, 2018).

Quantitative PCR (qPCR) was conducted using the QuantStudio 6 Pro Real-Time PCR System (ThermoFisher Scientific). The reactions were run with PowerUp SYBR Green Master Mix (ThermoFisher), along with forward and reverse primers designed to match either the experimental locus (DSB) on chromosome 7, or control locus (CTRL), on the *pre1* gene on chromosome 5, as described in Ferrari *et al*., 2018 (table 2.3). The DSB primers encompassed a region of DNA that was downstream of an AscI cut site and contained two Hyp188iii sites. The DNA region the CTRL primers encompassed did not include an Hpy188iii site, nor was it near an AscI site (details in section 3.2.5).

2.7.3 Analysis of qPCR

The data received from qPCR was analyzed using the Design & Analysis Software 2.6.0 (ThermoFisher). Each sample was edited in the software to be “Target 1”, which uses SYBR as the reporter and ROX as the passive dye. Both dyes are included in the PowerUp Green Master Mix (ThermoFisher). Once the “Analyze” function was executed, an amplification plot appeared with all the data from the samples in that run, which included the sample name, Ct score, Ct confidence, amp score, and amp status. The Ct score represents the number of cycles the sample took to reach above background noise. The confidence of this score is provided as a number between 0-1, where 1 indicates a greater reliability. The amp score indicates the quality of the

amplification curve, where the higher the amp score, the better quality the amplification is with more confidence. Lastly, the amp status can show as “amp”, such that the target amplified, “no amp”, suggesting no amplification of the target, or “inconclusive”, where the software is unable to determine if amplification occurred.

Ct scores were normalized to the fluorescence in CTRL and mock samples by calculating the ΔΔCt scores (described in section 3.2.5). Samples were additionally normalized to fluorescence of DNA before DSB induction began by subtracting the ΔΔCt of any given time point from the time 0 ΔΔCt to give the ΔC_q. The mean of 4 replicates was calculated for each time point, along with standard error of the mean (shown in section 3.2.5). Unpaired student’s t test was used to determine statistical significance with 95% confidence.

Chapter 3

Rif1 Interacts with Glc7 to Regulate DSB Repair Pathway Choice by Promoting Non-Homologous End Joining

3.1 Introduction

Faithful DNA replication and the prevention of events, such as senescence or cancer, is dependent on precise replication timing and the accurate and efficient repair of DNA DSBs. Along with replication timing, Rif1 has been recognized as a crucial actor in DSB repair pathway determination, seemingly promoting NHEJ. Our data suggests Rif1 works in conjunction with the protein phosphatase, Glc7, to promote NHEJ.

Rif1 contains a proline-rich motif (PPDSPP) in its C-terminal region, discovered by a previous member of the Duncker lab, Larasati (Larasati, 2020). This motif allows Dbf4, the regulatory subunit of DDK, to bind and DDK to phosphorylate Rif1, downregulating Rif1's interaction with Glc7, which prevents the inhibitory role of Rif1-Glc7 on the Mcm helicase (Kuntziger *et al*., 2006; Hiraga *et al*., 2014). Using a yeast two-hybrid analysis, Larasati found that *rif1* Δ*PPDSPP* was severely impaired in binding Dbf4. However, mutating the PPDSPP region did not significantly reduce the growth rate of cells in comparison to *RIF1* wild type cells. Additionally, a *rif1* Δ*PPDSPP* yeast strain did not exhibit any appreciable difference in sensitivity to genotoxic agents compared to wild type cells (Larasati, 2020).

Rif1 contains five potential CDK phosphorylation sites, three of which prime DDK phosphorylation (Hiraga *et al*., 2014). The literature has previously shown that CDK phosphorylation of Rif1 aids in the regulation of the interaction between Rif1 and Glc7 (Hiraga *et al*., 2014). Thus, in an attempt to disrupt CDK-mediated phosphorylation of Rif1, Larasati mutated these five residues to alanine (*rif1 5A*). However, Larasati found that, like the *rif1* Δ*PPDSPP* strain, the *rif1 5A* cells did not exhibit reduced cell growth nor change in sensitivity to

genotoxic agents in comparison to the parental wild type strain. Upon combining the *5A* and Δ*PPDSPP* mutations, cells grew poorly and demonstrated a delay in S phase entry. This strain was also exposed to a variety of genotoxic agents and demonstrated hypersensitivity when exposed to the DNA DSB-inducing agents, bleocin and phleomycin (figure 3.1). These results indicate that the DDK- and CDK-mediated phosphorylation of Rif1, thereby disrupting Rif1's interaction with Glc7, influences DNA replication initiation and resistance to genotoxic stress (Larasati, 2020).

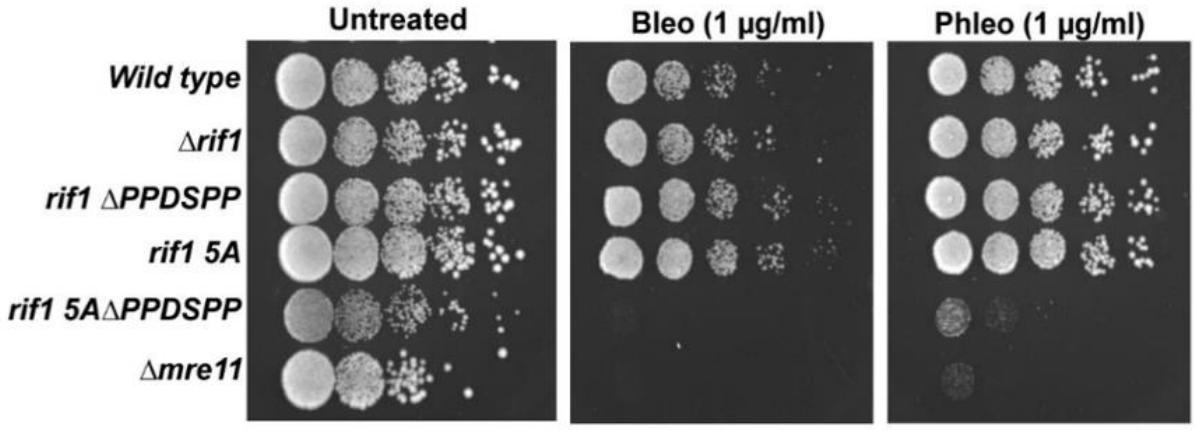

Figure 3.1. *rif1 5AΔPPDSPP* cells demonstrate hypersensitivity to the genotoxic agents, bleocin and phleomycin. Saturated cultures of yeast strains were serially diluted 10-fold and spotted onto YPD medium or YPD medium with bleocin or phleomycin at a concentration of 1µg/ml. Plates were incubated at 30°C and imaged after two days. The Δ*mre11* strain was used as a control that is known to be sensitive upon exposure to genotoxic agents (Ajimura *et al*., 1993) (figure was reproduced with permission from Larasati, 2020).

The important function of Rif1 in repair pathway choice at DNA DSBs had promoted Larasati to further investigate this. Larasati combined the *rif1 5A*Δ*PPDSPP* mutation with a deletion of a gene encoding a protein involved in the NHEJ repair pathway, *NEJ1*. Δ*nej1/rif1 5A*Δ*PPDSPP* cells demonstrated rescue of hypersensitivity upon exposure to the DNA DSB-inducing agents bleocin and phleomycin in comparison to *rif1 5A*Δ*PPDSPP* cells (figure 3.2). In contrast, no rescue of sensitivity was observed when the *rif1 5A*Δ*PPDSPP* mutation was combined with a deletion of either of two genes encoding proteins involved in HR, *SAE2* or *EXO1*. Additionally, an upregulation of NHEJ has been shown to be deleterious to cells due to its simple re-ligation, yet error-prone, mechanism, resulting in deletions or chromosome rearrangements (Seluanov *et al*., 2004). Taken together, Larasati's results demonstrated that disruption of the NHEJ pathway, but not HR, rescues genotoxic hypersensitivity in the *rif1 5A*Δ*PPDSPP* strain, and, therefore, the hypersensitivity seen in this strain is likely due to an upregulation of the NHEJ pathway (Larasati, 2020).

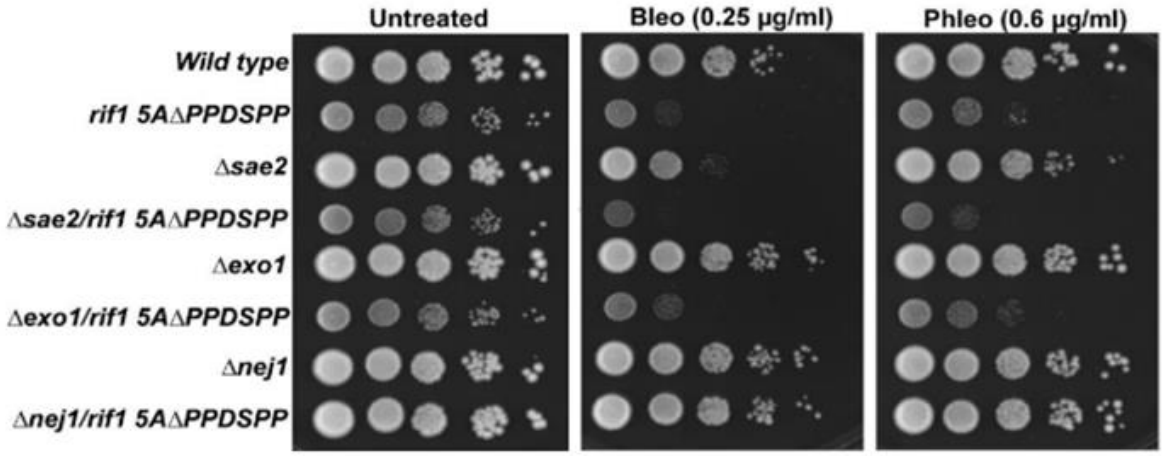

Figure 3.2. *rif1 5AΔPPDSPP* cells demonstrate rescue of hypersensitivity to genotoxic agents upon disrupting NHEJ repair pathway. Saturated cultures of yeast strains were serially diluted 10-fold and spotted onto YPD medium or YPD medium with bleocin or phleomycin at a concentration of 0.25 µg/ml and 0.6 µg/ml, respectively. Plates were incubated at 30°C and imaged after two days. The Δ*mre11* strain was used as a control that is known to be sensitive upon exposure to genotoxic agents (Ajimura *et al.*, 1993) (figure was reproduced with permission from Larasati, 2020).

After determining that the hypersensitivity seen in the *rif1 5A*Δ*PPDSPP* strain is likely due to an increase of NHEJ to repair DSBs, the next step was to investigate the cause of this increased genotoxicity in response to DSB-inducing agents. Since DDK cannot phosphorylate Rif1 to prevent its interaction with Glc7 in the *rif1 5A*Δ*PPDSPP* strain, it would be of great interest to determine if abrogating the interaction between Rif1 and Glc7 rescues hypersensitivity. The question that remained to be answered is: is the genotoxicity seen in *rif1*

5AΔPPDSPP cells due to Rif1's gain-of-function in constitutively maintaining its interaction with Glc7?

3.2 Results

3.2.1 Mutating the Rif1 RVxF/SILK motif partially rescues hypersensitivity of *rif1 5AΔPPDSPP*

Rif1 contains an RVxF/SILK motif in its N terminus, which is essential for facilitating its interaction with Glc7, as reported previously (Mattarocci *et al*., 2016). Recently, Larasati demonstrated that mutating the RVxF/SILK motif in the *rif1 5AΔPPDSPP* strain, partially rescued hypersensitivity to DSB-inducing agents (unpublished preliminary results). Therefore, the interaction between Rif1 and Glc7 appears to be, in part, a cause of the hypersensitivity seen in the *rif1 5AΔPPDSPP* strain.

According to our hypothesis, Rif1 interacts with Glc7 to counteract HR and promote NHEJ. Therefore, by abrogating the interaction between Rif1 and Glc7, there should be a decrease in NHEJ, and, thus, a promotion of HR as the DSB repair pathway of choice. Larasati had created the *rif1 RVxF/SILK* and *rif1 RVxF/SILK 5AΔPPDSPP* mutants to conduct spot plate assays. Upon spot plating these strains onto YPD medium containing various concentrations of phleomycin or bleocin, a rescue of hypersensitivity was observed upon mutating the RVxF/SILK motif in the *rif1 5AΔPPDSPP* strain.

To ensure these results were reproducible, I conducted this spot plate assay twice more with *WT Rif1*, *rif1 5AΔPPDSPP*, *rif1 RVxF/SILK*, *rif1 RVxF/SILK 5AΔPPDSPP* strains as well as a Δ*mre11* strain as a control known to be sensitive to genotoxic agents (Ajimura *et al*., 1993) (figure 3.3). All strains were plated as serial dilutions onto YPD medium or YPD medium containing phleomycin or zeocin at a concentration of 2 µg/ml or 4 µg/ml, and 4 µg/ml or 6 µg/ml, respectively. Consistent with what was seen the first time with Larasati's work, a partial rescue can be seen in the *rif1 RVxF/SILK 5AΔPPDSPP* strain compared to *rif1 5AΔPPDSPP*, which can still interact with Glc7. These results suggest that there is a role of Glc7 at DSBs in promoting NHEJ and causing hypersensitivity to genotoxic stress in the context of the *rif1 5AΔPPDSPP* mutant.

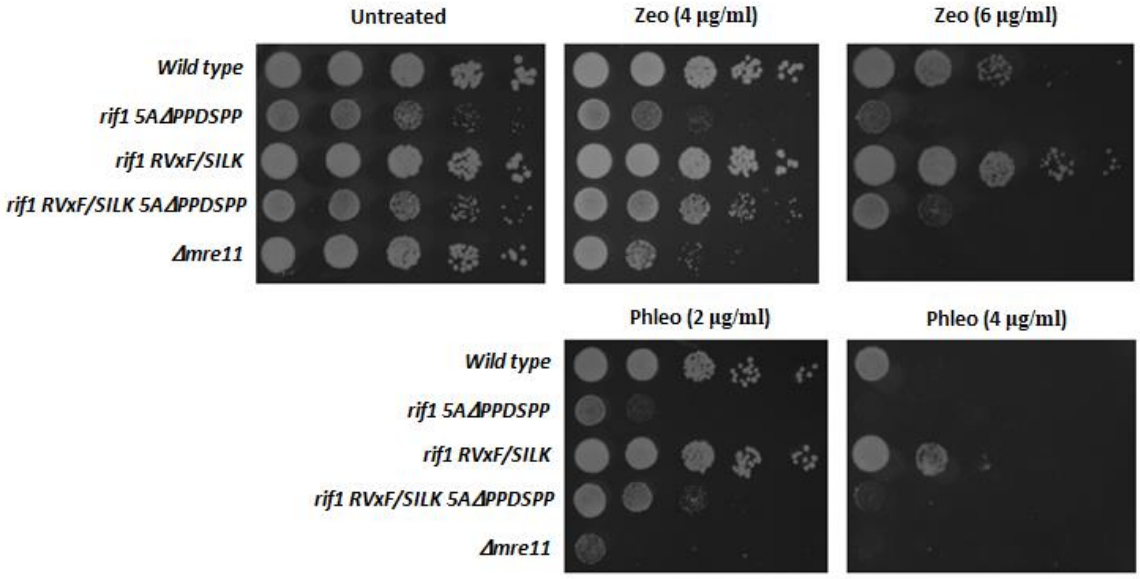

Figure 3.3. *rif1 5AΔPPDSPP* cells demonstrate hypersensitivity to genotoxic agents and show partial rescue when combined with the *RVxF/SILK* mutation. Saturated cultures of the indicated strains were serially diluted 10-fold and spotted onto YPD medium or YPD medium with zeocin or phleomycin at concentrations of 4 µg/ml and 6 µg/ml or 2 µg/ml and 4 µg/ml, respectively. Plates were incubated at 30°C and imaged after two days. The Δ*mre11* strain was used as a control that is known to be sensitive upon exposure to genotoxic agents (Ajimura *et al*., 1993). Three independent spot plate assays were performed; a representative image of one trial is shown.

3.2.2 Preventing S-palmitoylation of Rif1 by mutating residues C466 and C473 partially rescues hypersensitivity in *rif1 5AΔPPDSPP*

Following the observation of partial rescue of hypersensitivity to zeocin and phleomycin upon abrogating the RVxF/SILK motifs, we wanted to determine if we could rescue the *rif1 5AΔPPDSPP* strain further. Due to the importance of the Rif1 C466 and C473 residues for translocation of Rif1 to the inner nuclear membrane (Fontana *et al*., 2019), we first mutated these residues in *WT Rif1* and *rif1 5AΔPPDSPP* strains to assess whether preventing Rif1's normal nuclear localization would rescue hypersensitivity.

Mutating C466 and C473, to alanine was completed using CRISPR-Cas9 as described in the Materials and Methods chapter of this thesis. The results were as expected, as we can see a partial rescue of hypersensitivity upon mutating these cysteine residues in the *rif1 5AΔPPDSPP* strain (figure 3.4). These results suggest that Rif1 is required to be present at the DSB in order for the *rif1 5AΔPPDSPP* strain to demonstrate hypersensitivity, and thus, promote NHEJ, in response to genotoxic stress. Furthermore, this finding aids in the recent and novel literature that the C466 and C473 residues are essential for Rif1's function at DSBs. The *rif1 C466A/C473A* strain demonstrated a phenotype similar to *WT Rif1* with slightly better growth upon exposure to zeocin. This is semi-consistent with previous work which showed *rif1 C466A/C473A* cells demonstrated increased resistance to zeocin compared to wild type cells, indicating a disruption of NHEJ by the loss of these S-palmitoylation sites (Fontana *et al*., 2019).

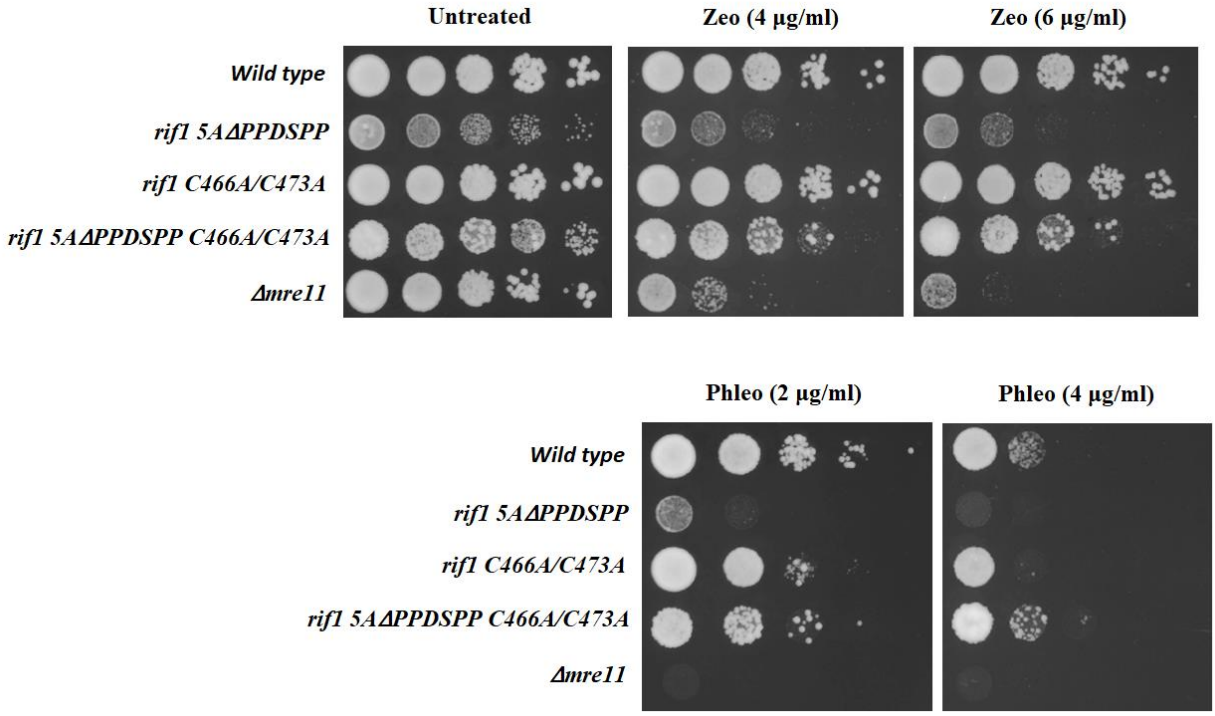

Figure 3.4. *rif1 5AΔPPDSPP* cells demonstrate partial rescue of hypersensitivity to genotoxic agents when combined with C466A and C473A mutations. Saturated cultures of the indicated strains were serially diluted 10-fold and spotted onto YPD medium or YPD medium with zeocin or phleomycin at concentrations of 4 µg/ml and 6 µg/ml, or 2 µg/ml and 4 µg/ml, respectively. Plates were incubated at 30°C and imaged after two days. The Δ*mre11* strain was used as a control that is known to be sensitive upon exposure to genotoxic agents (Ajimura *et al*., 1993). Three independent spot plate assays were performed; a representative image of one trial is shown.

3.2.3 Introduction of C466A and C473A mutations does not further rescue hypersensitivity in a *rif1 RVxF/SILK 5AΔPPDSPP* strain

After observing rescue in the *rif1 5AΔPPDSPP* strain upon adding the C466A and C473A mutations, an additional strain was created using CRISPR-Cas9 by myself and an undergraduate student in the Duncker lab, Karan Patel, in which these S-acylation sites were mutated in the *rif1 RVxF/SILK 5AΔPPDSPP* strain. The rationale behind creating this strain was to assess if combining these mutations, whereby we abrogate the interaction between Rif1 and Glc7, and prevent Rif1 from localizing to DSBs, will further rescue *rif1 5AΔPPDSPP* strain hypersensitivity to DSBs. In the *rif1 RVxF/SILK 5AΔPPDSPP* strain, Rif1 remains able to translocate to the inner nuclear membrane and bind to DNA ends at the DSB. We, therefore, sought to investigate if there is an additional effect on sensitivity to genotoxic stress, such that Rif1 has an independent role at DSBs whereby it must be present at the break, as well as a role with Glc7 to promote NHEJ. If no additional effect is seen, this would suggest there is no additional independent role of Rif1 at DSBs without Glc7 that would rescue hypersensitivity further in the *rif1 5AΔPPDSPP* strain. Conversely, if there is additional rescue of hypersensitivity, such that the addition of C466A and C473A mutations rescues hypersensitivity further in the *rif1 RVxF/SILK 5AΔPPDSPP* strain, this may suggest that Rif1 makes separate contributions, on its own and in conjunction with Glc7, to promote NHEJ at DSBs in the *rif1 5AΔPPDSPP* strain. Since a previous study had demonstrated that the ability of Rif1 to promote NHEJ was independent of Glc7 recruitment to DSBs (Mattarocci *et al*., 2017), it was hypothesized that we would observe additional rescue upon combining the RVxF/SILK and

C466A/C473A mutations in a *rif1 5AΔPPDSPP* strain. Surprisingly, in comparison to *rif1 RVxF/SILK 5AΔPPDSPP*, no additional rescue of hypersensitivity was observed upon adding the C466A and C473A mutations (figure 3.5). These results suggest that the hypersensitivity seen in the *rif1 5AΔPPDSPP* strain is, in part, due to the interaction between Rif1 and Glc7, with no additional effect of Rif1 at DSBs to promote NHEJ further than Rif1-Glc7 working in conjunction.

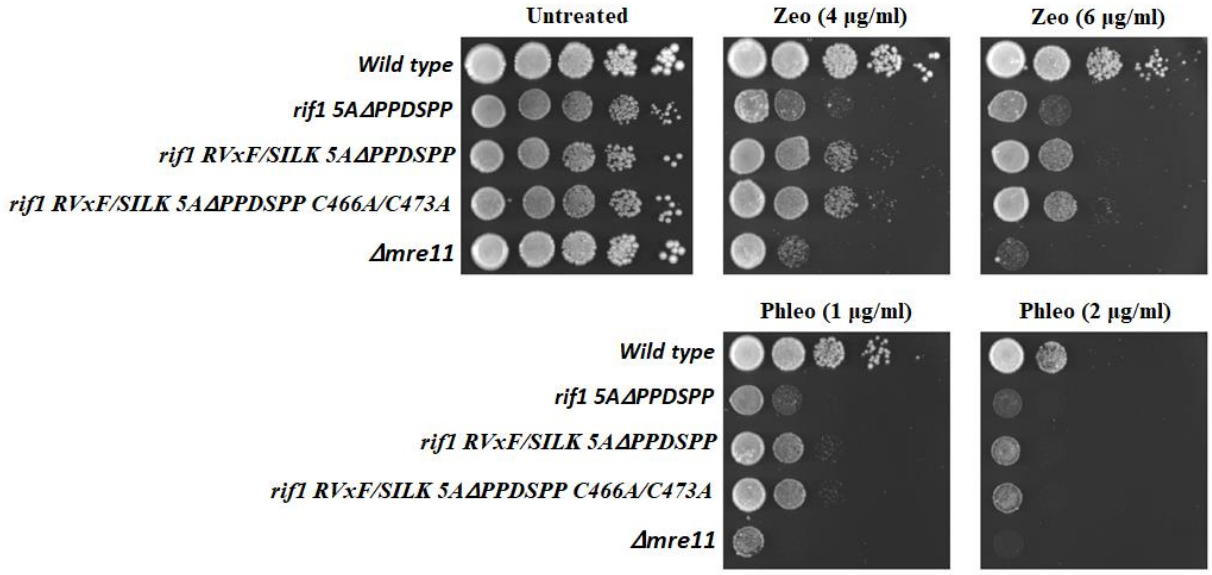

Figure 3.5. *rif1 RVxF/SILK 5AΔPPDSPP* cells demonstrate no additional rescue of hypersensitivity when combined with C466A and C473A mutations. Saturated cultures of the indicated strains were serially diluted 10-fold and spotted onto YPD medium or YPD medium with zeocin or phleomycin at concentrations of 4µg/ml and 6µg/ml, or 1µg/ml and 2µg/ml, respectively. Plates were incubated at 30°C and imaged after two days. The Δ*mre11* strain was

used as a control that is known to be sensitive upon exposure to genotoxic agents (Ajimura *et al*., 1993). Three independent spot plate assays were performed; a representative image of one trial is shown.

3.2.4 Preventing physical binding of Rif1 to DNA ends by mutating the Rif1 HOOK domain partially rescues hypersensitivity in a *rif1 5AΔPPDSPP* strain

To investigate the effects of Rif1 being able to physically bind to DNA ends in the *rif1 5AΔPPDSPP* strain, we used CRISPR-Cas9 to generate two additional strains where the lysine residues, K437, K563 and K570, were mutated to glutamic acid, as described in an earlier study (Mattarocci *et al*., 2017). These mutations were added to *WT Rif1* and *rif1 5AΔPPDSPP* strains to generate $Rif1_{HOOK}$ and $rif1_{HOOK}$ *5AΔPPDSPP* strains, respectively. According to our hypothesis, we expect to see rescue of hypersensitivity to DSBs in the $rif1_{HOOK}$ *5AΔPPDSPP* strain compared to *rif1 5AΔPPDSPP,* as we presume that Rif1's ability to physically bind DNA ends contributes to the hypersensitivity seen in the *rif1 5AΔPPDSPP* strain. Consistent with our hypothesis, we observe partial rescue in the $rif1_{HOOK}$ *5AΔPPDSPP* strain (figure 3.6).

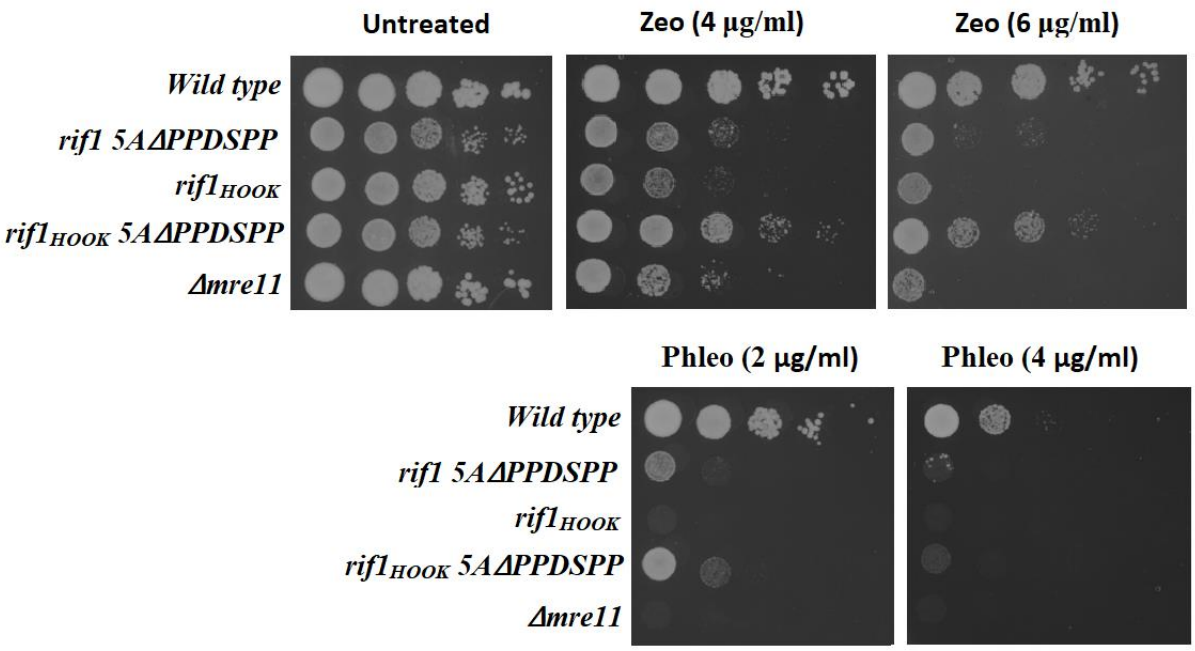

Figure 3.6. *rif1 5AΔPPDSPP* cells demonstrate partial rescue of hypersensitivity to genotoxic agents when combined with K437E, K563E and K570E mutations in the HOOK domain of Rif1. Saturated cultures of the indicated strains were serially diluted 10-fold and spotted onto YPD medium or YPD medium with zeocin or phleomycin at concentrations of 4µg/ml and 6µg/ml, or 2µg/ml and 4µg/ml, respectively. Plates were incubated at 30°C and imaged after two days. The Δ*mre11* strain was used as a control that is known to be sensitive upon exposure to genotoxic agents (Ajimura *et al*., 1993). Three independent spot plate assays were performed; a representative image of one trial is shown.

Interestingly, hypersensitivity to both zeocin and phleomycin can be seen in the *rif1*$_{HOOK}$ strain, which is contrary to the literature, as this mutation has been shown to result in defective

NHEJ upon DSB induction by HO endonuclease and increased cell survival upon exposure to zeocin (Mattarocci *et al*., 2017; Fontana *et al*., 2019). The cause of the hypersensitivity observed in the experiments reported here may be a result of off-target mutations due to the use of CRISPR-Cas9 to generate this strain. To test this result, spot plate assays were conducted including the *rif1*$_{HOOK}$ strain transformed with a plasmid expressing full-length (FL) *RIF1* under a CYC1 promoter (pCM Rif1 Myc). If the *rif1*$_{HOOK}$ strain expressing plasmid-encoded FL *RIF1* phenocopies *WT Rif1*, we can assume there are no off-target mutations. On the other hand, if the episomal expression of FL *RIF1* does not rescue hypersensitivity in the *rif1*$_{HOOK}$ strain generated in this study, this would suggest off-target mutations. The precursor plasmid of pCM Rif1 Myc, pCM190-myc13, is identical to pCM Rif1 Myc, but does not include FL *RIF1*. The *WT Rif1* and *rif1*$_{HOOK}$ strains underwent lithium acetate transformation to include either pCM190-myc13 or pCM Rif1 Myc and were grown on SC -ura containing phleomycin or zeocin, along with a Δ*mre11* strain, as both plasmids and the Δ*mre11* strain contain a URA3 selectable marker (figure 3.7). *rif1*$_{HOOK}$ with FL *RIF1* (pCM Rif1 Myc) phenocopied *rif1*$_{HOOK}$ with empty vector (pCM190-myc13). These preliminary results, obtained from one experiment, suggest that off-target mutation(s) in the *rif1*$_{HOOK}$ strain are the likely cause of the unusual phenotype observed in the previous spot plate assay (figure 3.6). These results are preliminary as expression of Rif1 in the transformed plasmids had yet to be confirmed.

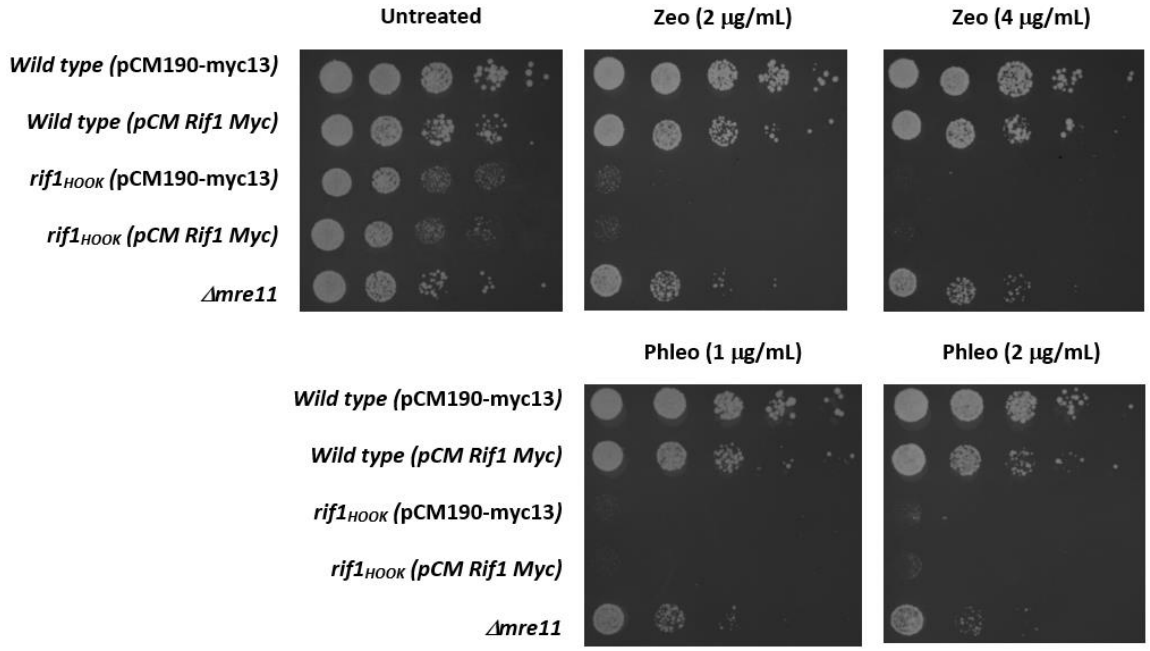

Figure 3.7. *rif1*$_{HOOK}$ cells fail to phenocopy *WT Rif1* upon exposure to genotoxic agents when transformed with a full-length *RIF1* expression construct. Saturated cultures of the indicated strains were serially diluted 10-fold and spotted onto SC -ura medium or SC -ura medium with zeocin or phleomycin at concentrations of 2μg/ml and 4μg/ml, or 1μg/ml and 2μg/ml, respectively. Plates were incubated at 30°C and imaged after two days. The Δ*mre11* strain was used as a control that is known to be sensitive upon exposure to genotoxic agents (Ajimura *et al*., 1993). One spot plate assay was performed.

3.2.5 *rif1 5AΔPPDSPP* favours NHEJ over HR in DNA DSB repair, compared to *WT Rif1*

To examine whether the *rif1 5AΔPPDSPP* strain promotes NHEJ over HR in DNA DSB repair, a resection assay was conducted using a qPCR-based assay. Relative resection to the wild type strain was measured, where ΔC_q scores were used as a proxy for repair pathway choice, as described below. The integrative pRG645lexO-AscI_LexA-TF_LEU2MX plasmid was added to both *WT Rif1* and *rif1 5AΔPPDSPP* strains, to generate yeast strains DY-418 and DY-419, as described in the Materials and Methods chapter of this thesis. The integrative plasmid contained an engineered transcription factor comprised of the estrogen receptor domain, LexA, and a transactivation domain, B112. This factor is constitutively expressed and translocated to the nucleus in the presence of estrogen. Once in the nucleus, it binds to an engineered promoter consisting of LexA binding sites and fused to yeast CYC1 core promoter (P_{lexO}) to drive target gene expression. Under the transcriptional control of this promoter is the AscI restriction enzyme gene. Therefore, when estrogen is present, the AscI restriction enzyme is expressed and can cut at specific sites throughout the genome. Cultures (~5x10^5cells/ml) were induced with 2μM β-estradiol for 6 hours, collecting samples at 2-hour intervals (see section 2.7 for details). Following genomic extraction, DNA was either mock-digested or digested with Hpy188iii restriction enzyme. The "DSB" primers used encompassed a region downstream of an AscI cut site and with Hpy188iii cut sites in between (figure 3.8). Control "CTRL" primers on a different chromosome were also used, which encompassed a region that did not contain an Hpy188iii cut site nor was it located near an AscI cut site. The complementary sequence to the primers

downstream of the AscI cut site may be resected depending on if the cell uses NHEJ or HR to repair the break.

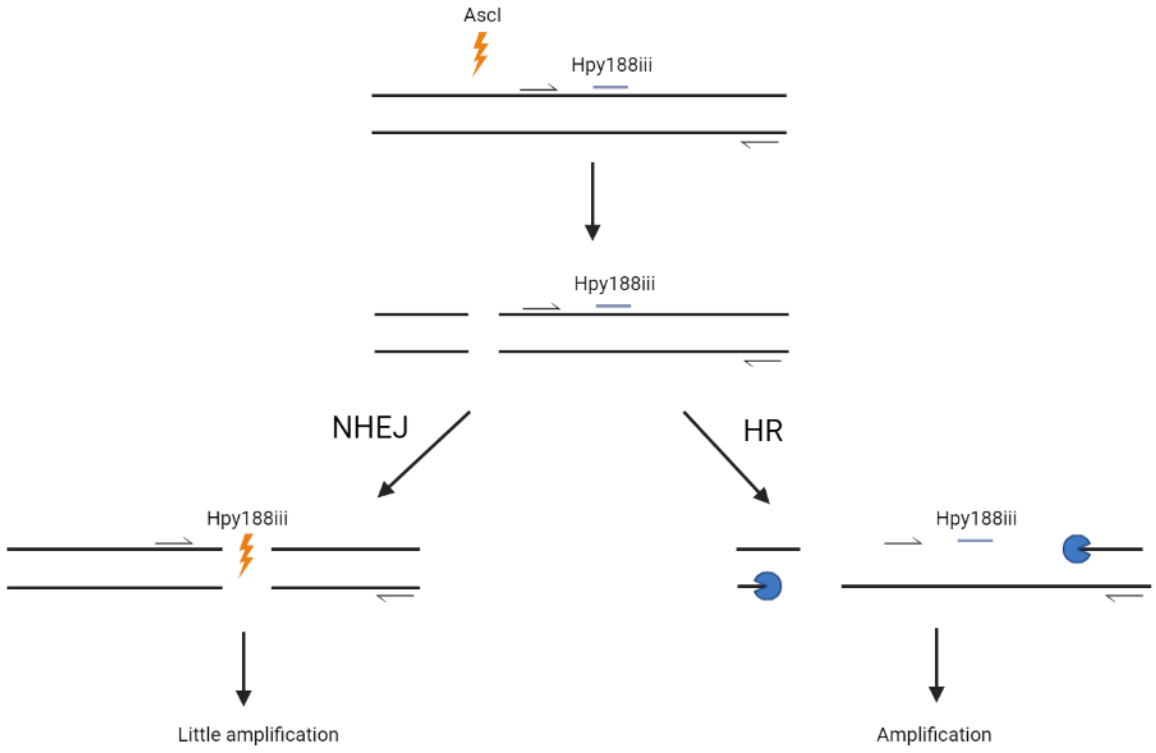

Figure. 3.8. Schematic representation of qPCR-based resection assay. As shown in the figure, the AscI restriction enzyme creates a DSB upstream of the primers encompassing a region including an Hpy188iii site. If the cell relies on NHEJ to repair the DSB induced by AscI, Hpy188iii will cut the DNA in between the primers, disrupting PCR primers from amplifying the DNA region. If the cell relies on HR to repair the AscI-induced DSB, the DNA becomes single-stranded due to resection of the DNA ends, and Hpy188iii will not be able to cleave the DNA, allowing the PCR primers to amplify a greater region of DNA.

If the cell uses NHEJ, the DNA will be repaired without the extensive resection that occurs with HR, and Hpy188iii can cut the double-stranded DNA, therefore allowing less DNA to be amplified. If HR is used to repair the AscI cut site, there will be resection of one strand, and, thus, Hpy188iii will not be able to cleave the DNA as its recognition site will be single stranded. In this case, the primers can still bind to the DNA, and the amplification of DNA should take less cycles to fluoresce above background noise than the cells that repair the DSB using NHEJ. The Ct score represents the number of cycles it takes for the fluorescence of the sample to reach above the background signal. Therefore, a lower Ct score would be indicative of more DNA being amplified and suggests the cell repaired the AscI cut using HR. In contrast, a higher Ct score would suggest NHEJ. For this purpose, ΔC_q scores were used as a proxy of repair pathway, which is calculated utilizing the following equations (Ferrari *et al*., 2018; Gnügge & Symington, 2020):

$$\Delta\text{Ct digested} = \text{Ct digested DSB} - \text{Ct digested CTRL}$$

$$\Delta\text{Ct mock} = \text{Ct mock DSB} - \text{Ct mock CTRL}$$

$$\Delta\Delta\text{Ct} = \Delta\text{Ct digested} - \Delta\text{Ct mock}$$

$$\Delta C_q = \Delta\Delta\text{Ct } t_0 - \Delta\Delta\text{Ct } t_{evaluated}$$

Statistical analysis was completed for the resection assay by calculating ΔC_q scores and using two sample t test with equal variances. Variance was determined using an F statistic for variance. On average, *WT Rif1* experiences a lower ΔC_q score than *rif1 5AΔPPDSPP* 6 hours

post-induction (figure 3.9). The difference seen at this time interval is statistically significant with a p-value less than 0.05 and we can reject the null hypothesis. Therefore, our findings suggest *rif1 5AΔPPDSPP* favors NHEJ 6 hours post-treatment in comparison to *WT Rif1*. These results agree with our hypothesis and our findings with the spot plate assays that Rif1 and Glc7 work together in the *rif1 5AΔPPDSPP* strain to promote NHEJ.

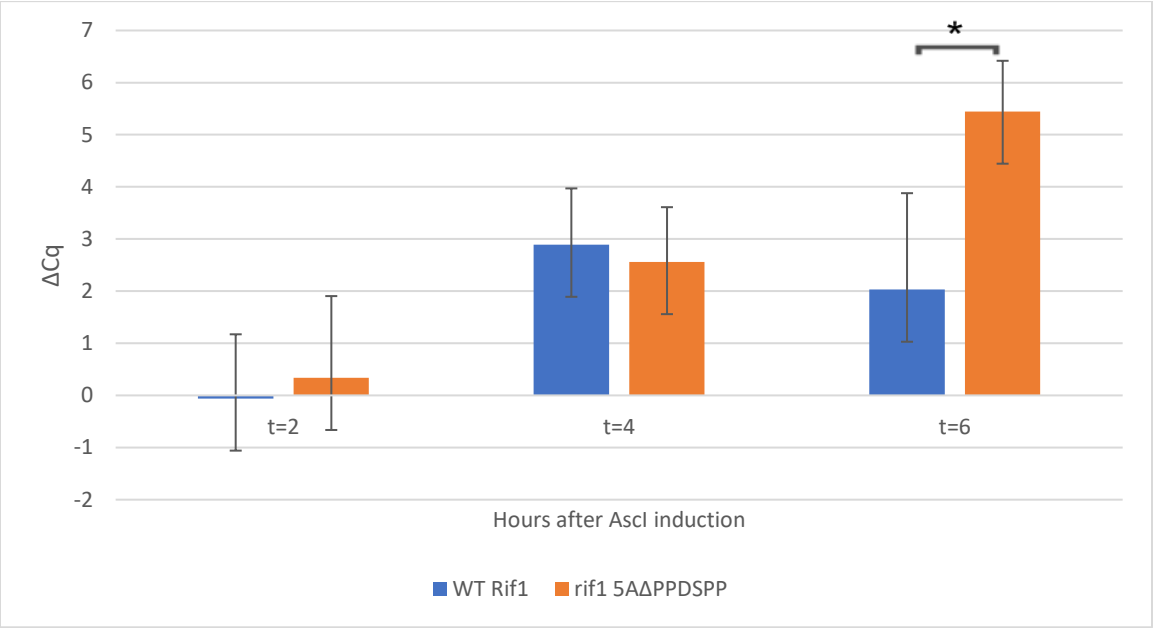

Figure 3.9. Comparison of ΔC_q scores suggests *rif1 5AΔPPDSPP* favors NHEJ to repair DSBs in comparison to *WT Rif1*. Graph indicates ΔC_q scores of *WT Rif1* and *rif1 5AΔPPDSPP* using a qPCR-based resection assay, adapted from Ferrari *et al*., 2018. The error bars represent standard error of the mean of four biological replicates. Significance was determined using two-tailed, unpaired Student's t-test assuming equal variances. *$p < 0.05$.

Student's t-test was used to produce a p-value and provide confidence for these results. A 95% confidence level was used for the hypothesis. Described below is the null hypothesis (H_0) and the alternative hypothesis (H_a).

H_0 = The mean of *rif1 5A*Δ*PPDSPP* ΔC_q scores did not significantly differ compared to *WT Rif1*

H_a = The mean of *rif1 5A*Δ*PPDSPP* ΔC_q scores did significantly differ compared to *WT Rif1*

Table 3.1. Resection Assay p-values for *WT Rif1* vs *rif1 5A*Δ*PPDSPP* at Differing Time Points After DSB Induction

	***WT Rif1* vs *rif1 5A*Δ*PPDSPP* t=2**	***WT Rif1* vs *rif1 5A*Δ*PPDSPP* t=4**	***WT Rif1* vs *rif1 5A*Δ*PPDSPP* t=6**
Mean *WT Rif1*	-0.059	2.891	0.232
Mean *rif1 5A*Δ*PPDSPP*	0.336	2.559	5.445
Variance *WT Rif1*	6.066	4.663	13.685
Variance *rif1 5A*Δ*PPDSPP*	9.843	4.427	3.796
Degrees of Freedom	6	6	6

t-value	-0.198	0.221	-2.494
p-value	0.849	0.833	0.047

The null hypothesis was not rejected for *WT Rif1* vs *rif1 5AΔPPDSPP* comparisons at 2- and 4-hours post-induction, but was rejected for t=6, as the p-value was less than 0.05. The p-value at 6-hours post-induction is 0.047, indicated in table 3.1. Since the p-value is less than 0.05, this finding is statistically significant. These results suggest that there is a difference between *WT Rif1* and *rif1 5AΔPPDSPP* in which repair pathway choice they favor 6 hours after DSBs occur.

Chapter 4

General Conclusions and Future Directions

4.1 The interaction between Rif1 and Glc7 is sufficient in promoting NHEJ at DNA DSBs

Both Rif1 and PP1 interact with a vast and diverse number of proteins, implicated in numerous cellular processes and pathways. The relationship between Rif1 and PP1 has been demonstrated in many organisms, whereby they influence a multitude of events in the cell, including DNA replication, abscission timing, and the suppression of telomere extension (Armstrong *et al*., 2020; Hiraga *et al*., 2014; Bhowmick *et al*., 2019; Kedziora *et al*., 2018). Recently, Rif1 and PP1 have been discovered to be involved in the regulation of DNA DSB repair pathway choice, seemingly favouring NHEJ under genotoxic conditions (Isobe *et al*., 2021; Garzón *et al*., 2019).

The Rif1 PPDSPP motif facilitates its interaction with the Dbf4 subunit of DDK, and subsequent phosphorylation by DDK, allowing Rif1 to be phosphorylated near the motif where it interacts with Glc7, RVxF/SILK. Additionally, Rif1 has 5 CDK-mediated phosphorylation sites near the RVxF/SILK motif. Mutation of these phosphorylation sites resulted in this *rif1 5AΔPPDSPP* strain demonstrating poor growth, an S phase entry delay and sensitivity to genotoxic stress, specifically to DSB-inducing agents (Larasati, 2020). Various spot plate assays revealed a relationship between Rif1 and Glc7 in influencing cellular recovery to DNA DSBs. Moreover, the RVxF/SILK motif was mutated, thus, preventing the interaction between Rif1 and Glc7, to determine if their action together is contributing to the hypersensitive phenotype seen in *rif1 5AΔPPDSPP* in response to genotoxic agents. A partial rescue of hypersensitivity was seen

upon abrogating their interaction. Therefore, Rif1 and Glc7 act together to not only have implications in replication timing, but also in the response to genotoxic stress.

Furthermore, two Rif1 cysteine residues, C466 and C473, which facilitate localization of Rif1 to the inner nuclear membrane via S-palmitoylation, and three Rif1 lysine residues, K437, K563, and K570, which allow for the physical binding of Rif1 to DNA ends, were mutated and combined with the *rif1 5AΔPPDSPP* strain. Both sets of mutations resulted in partial rescue of hypersensitivity, therefore, suggesting both the localization and physical binding of Rif1 to DNA is important for Rif1-Glc7 in promoting NHEJ as the repair pathway for DSBs. Interestingly, upon combining the *rif1 RVxF/SILK 5AΔPPDSPP* strain with the C466A and C473A mutations, no additional rescue was observed (figure 3.5). Since there was no difference in hypersensitivity between the strains containing the two types of mutation (i.e., RVxF/SILK or C466A/C473A on their own) and a combination of these (i.e., both RVxF/SILK and C466A/C473A), these results suggest that any independent role of Rif1 does not further rescue hypersensitivity beyond the joint action of Rif1 and Glc7 together at DSBs in the *rif1 5AΔPPDSPP* strain. An interesting aspect that should be considered is the effect Rif1 has, if any, on luminal DSBs. Mutating the S-palmitoylation sites, C466 and C473, prevents the localization of Rif1 to the periphery of the nucleus. However, Rif1 has been found to have a nuclear localization signal in Hela cells, a C-terminal KKRK motif, suggesting Rif1 may be able to, not only bind to peripheral DSBs, but luminal DSBs, as well (Li *et al*., 2007). Further investigations should be conducted mutating the Rif1 nuclear localization signal to determine the effect, if any, of Rif1 at DSBs located in the lumen of the nucleus when Rif1-Glc7 activity is upregulated.

4.2 A resection-based assay reveals a decrease in resection in *rif1 5AΔPPDSPP* compared to *WT Rif1*

A qPCR-based resection assay was conducted to evaluate DNA end resection in response to induced DSBs in the *rif1 5AΔPPDSPP* strain in comparison to *WT Rif1*. The rationale behind this assay was to confirm the hypersensitive phenotype seen in the *rif1 5AΔPPDSPP* strain in response to genotoxic stress is due to an increase in repair by NHEJ, as opposed to HR. The qPCR-based resection assay was conducted using the *lexO-AscI* system (Gnügge & Symington, 2020). Consistent with the above results and literature proposing Rif1 as a component of NHEJ, we found that the *rif1 5AΔPPDSPP* strain influences repair pathway choice in a way such that it reduces the cell's ability to use HR. Interestingly, the *rif1 5AΔPPDSPP* strain, 6-hours after DSBs were induced, resulted in the highest number of Ct cycles required to amplify the DNA above background noise, taking into account amplification of the mock, control, and time 0 samples (ΔC_q). This strain produced a statistically significant higher ΔC_q score 6-hours post-DSB induction in comparison to *WT Rif1*. These results suggest that the mechanism by which Rif1 and Glc7 act to promote NHEJ and cause hypersensitivity to genotoxic stress is through preventing the formation of ssDNA, and, thus, preventing the cell from repairing DSBs via HR.

4.3 Future directions and implications

The research conducted in this thesis solidifies prior evidence and expands current knowledge of Rif1 and its interaction with Glc7 in its regulatory role at DNA DSBs under genotoxic conditions. As Rif1 and PP1, both together and independently, have oncogenic roles,

including the promotion of tumor growth and cancer stem cell-like properties, research in this area contributes to the advancement of targeted therapies directed at Rif1 and PP1 (Mei *et al*., 2018a; Mei *et al*., 2018b; Caron *et al*., 2019). The data presented in this thesis contributes to the growing knowledge of Rif1 in influencing which repair pathways are favoured to fix DSBs and which proteins Rif1 interacts with to have its effect. A few immediate goals following this work include investigating candidate proteins, as well as proteins found to be differentially phosphorylated in the strains indicated in this thesis, that Rif1 and Glc7 may interact with to promote NHEJ upon exposure to DSB-inducing agents. Specifically, Rif1 and PP1 in mammalian cells have been found to work together to dephosphorylate WRN helicase, the homolog of yeast Sgs1, and Dna2 (Mukherjee *et al*., 2019; Garzón *et al*., 2019). Both Sgs1 and Dna2 are known to be involved in repair of DSBs by HR. Therefore, it would be of great interest to determine whether Sgs1 and Dna2 are differentially phosphorylated in *WT Rif1* and *rif1 5AΔPPDSPP* yeast strains. Such a project has recently been initiated by myself and an undergraduate student working in the Duncker lab, Karan Patel, whereby DNA sequence encoding 3x HA tags are being added to the *SGS1* and *DNA2* genes in both *WT Rif1* and *rif1 5AΔPPDSPP* strains for Western blotting experiments to visualize these proteins. If these proteins are differentially phosphorylated, we may see a difference in mass upon visualization of the blot, using a primary anti-HA antibody. The aim of this study is to provide mechanistic evidence of Rif1-Glc7 promoting NHEJ through the dephosphorylation of proteins involved in the HR repair pathway.

Additionally, a project focused on a more general perspective would allow for the identification of novel protein targets at DNA DSBs, which may be dephosphorylated by Rif1-Glc7. In this approach, chromatin immunoprecipitation and mass spectrometry would be utilized to identify proteins, and their specific residues, differentially phosphorylated in *WT Rif1* and *rif1 5A*Δ*PPDSPP*. Specifically, we would subject cells to a DSB-inducing agent and use a cross-linking agent, such as formaldehyde, to preserve any interactions. Cells would be spheroplasted to remove the cell wall, and DNA would be sonicated to generate ~500 bp fragments, in which antibodies directed at Ku70, a protein that binds to DNA ends, would be used. Next, NaCl would be used to reverse the cross-linking agent, and the samples would be treated with DNase, to aid in the extraction of proteins. The samples would be analyzed by mass spectrometry to identify proteins that are differentially phosphorylated in the various strains. Phosphomimetic mutations would be introduced to residues that are found to be differentially phosphorylated in identified proteins and spot plate assays would be conducted to assess the indicated strains' ability to rescue hypersensitivity under genotoxic conditions. These results would shed light on mechanistic details of Rif1 and Glc7 in their ability to promote NHEJ upon exposure to DSB-inducing agents, such as phleomycin and zeocin.

To further strengthen the results of the resection assay, a couple of downstream experiments should be considered. Firstly, the difference seen between *WT Rif1* and *rif1 5A*Δ*PPDSPP* was only statistically significant after 6 hours of DSB induction. It would be of interest to determine if the effect seen continues after the 6-hour mark, such as up to 8-hours post-induction. Secondly, including the *rif1 RVxF/SILK 5A*Δ*PPDSPP* strain, where the

interaction between Rif1 and Glc7 is abrogated, would solidify the evidence that their interaction is causing the prevention of ssDNA accumulation, and, thus, promoting NHEJ. Such revelations would enhance the current pursuit of targeting Rif1 for cancer therapeutics and progress in the field of targeted therapy.

Taken together, the results presented in this thesis support a model whereby Rif1 promotes repair by NHEJ in response to DSBs and uncovers mechanistic details of Rif1-Glc7 in their influence on repair pathway choice. Advancement in this research area contributes to the fundamental understanding of key aspects of cell survival, including faithful DNA replication and the repair of toxic DSBs through the Rif1-PP1 interaction, an interaction of which has been shown to be upregulated in a variety of cancers (Mei *et al*., 2017; Mei *et al*., 2018a; Caron *et al*., 2019).

Bibliography

Aggen, J. B., Nairn, A. C., & Chamberlin, R. (2000). Regulation of protein phosphatase-1. *Chemistry & biology*, *7*(1), R13–R23.

Ajimura, M., Leem, S. H., & Ogawa, H. (1993). Identification of new genes required for meiotic recombination in Saccharomyces cerevisiae. *Genetics*, *133*(1), 51–66.

Alver, R. C., Chadha, G. S., Gillespie, P. J., & Blow, J. J. (2017). Reversal of DDK-Mediated MCM Phosphorylation by Rif1-PP1 Regulates Replication Initiation and Replisome Stability Independently of ATR/Chk1. *Cell reports*, *18*(10), 2508–2520.

Armstrong, R. L., Das, S., Hill, C. A., Duronio, R. J., & Nordman, J. T. (2020). Rif1 Functions in a Tissue-Specific Manner To Control Replication Timing Through Its PP1-Binding Motif. *Genetics*, *215*(1), 75-87.

Balasubramanian, S., Andreani, M., Andrade, J. G., Saha, T., Sundaravinayagam, D., Garzón, J., … Di Virgilio, M. (2022). Protection of nascent DNA at stalled replication forks is mediated by phosphorylation of RIF1 intrinsically disordered region. *eLife*, *11*, e75047.

Bennett, J. M., & Reich, S. D. (1979). Bleomycin. *Annals of internal medicine*, *90*(6), 945–948.

Bhowmick, R., Thakur, R. S., Venegas, A. B., Liu, Y., Nilsson, J., Barisic, M., & Hickson, I. D. (2019). The RIF1-PP1 Axis Controls Abscission Timing in Human Cells. *Current biology: CB*, *29*(7), 1232–1242.e5.

Böhm, S., & Buchberger, A. (2013). The budding yeast Cdc48(Shp1) complex promotes cell cycle progression by positive regulation of protein phosphatase 1 (Glc7). *PloS one*, *8*(2), e56486.

Bollen, M., Peti, W., Ragusa, M. J., & Beullens, M. (2010). The extended PP1 toolkit: designed to create specificity. *Trends in biochemical sciences*, *35*(8), 450–458.

Bolotin-Fukuhara, M., Dumas, B., & Gaillardin, C. (2010). Yeasts as a model for human diseases. *FEMS Yeast Research*, *10*(8), 959–960.

Brandsma, I., & Gent, D. C. (2012). Pathway choice in DNA double strand break repair: observations of a balancing act. *Genome integrity*, *3*(1), 9.

Buonomo, S. B., Wu, Y., Ferguson, D., & de Lange, T. (2009). Mammalian Rif1 contributes to replication stress survival and homology-directed repair. *The Journal of cell biology*, *187*(3), 385–398.

Burgess, S. M., Powers, T., & Mell, J. C. (2017). Budding Yeast Saccharomyces Cerevisiae as a Model Genetic Organism. In ELS (pp. 1–12).

Cannon, J. F., Pringle, J. R., Fiechter, A., & Khalil, M. (1994). Characterization of glycogen-deficient glc mutants of Saccharomyces cerevisiae. *Genetics*, *136*(2), 485–503.

Caron, M. C., Sharma, A. K., O'Sullivan, J., Myler, L. R., Ferreira, M. T., Rodrigue, A., … Masson, J. Y. (2019). Poly(ADP-ribose) polymerase-1 antagonizes DNA resection at double-strand breaks. *Nature communications*, *10*(1), 2954.

Chapman, J. R., Barral, P., Vannier, J. B., Borel, V., Steger, M., Tomas-Loba, A., Sartori, A. A., Adams, I. R., Batista, F. D., & Boulton, S. J. (2013). RIF1 is essential for 53BP1-dependent nonhomologous end joining and suppression of DNA double-strand break resection. *Molecular cell*, *49*(5), 858–871.

Chen, J., Ghorai, M. K., Kenney, G., & Stubbe, J. (2008). Mechanistic studies on bleomycin-mediated DNA damage: multiple binding modes can result in double-stranded DNA cleavage. *Nucleic acids research*, *36*(11), 3781–3790.

Cohen P. T. (2002). Protein phosphatase 1--targeted in many directions. *Journal of cell science*, *115*(Pt 2), 241–256.

Cole, M. P., Jones, C. T., & Todd, I. D. (1971). A new anti-oestrogenic agent in late breast cancer. An early clinical appraisal of ICI46474. *British journal of cancer*, *25*(2), 270–275.

Cortez D. (2015). Preventing replication fork collapse to maintain genome integrity. *DNA repair*, *32*, 149–157.

Costanzo, M., Nishikawa, J. L., Tang, X., Millman, J. S., Schub, O., Breitkreuz, K., Dewar, D., Rupes, I., Andrews, B., & Tyers, M. (2004). CDK activity antagonizes Whi5, an inhibitor of G1/S transcription in yeast. *Cell, 117*(7), 899–913.

Davé, A., Cooley, C., Garg, M., & Bianchi, A. (2014). Protein phosphatase 1 recruitment by Rif1 regulates DNA replication origin firing by counteracting DDK activity. *Cell reports, 7*(1), 53–61.

de Bruin, R. A., McDonald, W. H., Kalashnikova, T. I., Yates, J., 3rd, & Wittenberg, C. (2004). Cln3 activates G1-specific transcription via phosphorylation of the SBF bound repressor Whi5. *Cell, 117*(7), 887-898.

DeCesare, J. M., & Stuart, D. T. (2012). Among B-type cyclins only CLB5 and CLB6 promote premeiotic S phase in Saccharomyces cerevisiae. *Genetics, 190*(3), 1001–1016.

Delacôte, F., Deriano, L., Lambert, S., Bertrand, P., Saintigny, Y., & Lopez, B. S. (2007). Chronic exposure to sublethal doses of radiation mimetic Zeocin selects for clones deficient in homologous recombination. *Mutation research, 615*(1-2), 125–133.

Duina, A. A., Miller, M. E., & Keeney J. B. (2014). Budding yeast for budding geneticists: a primer on the Saccharomyces cerevisiae model system. *Genetics, 197*(1), 33-48.

Escribano-Díaz, C., Orthwein, A., Fradet-Turcotte, A., Xing, M., Young, J. T., Tkáč, J., … Durocher, D. (2013). A cell cycle-dependent regulatory circuit composed of 53BP1-RIF1 and BRCA1-CtIP controls DNA repair pathway choice. *Molecular cell*, *49*(5), 872–883.

Feng, Z. H., Wilson, S. E., Peng, Z. Y., Schlender, K. K., Reimann, E. M., & Trumbly, R. J. (1991). The yeast GLC7 gene required for glycogen accumulation encodes a type 1 protein phosphatase. *The Journal of biological chemistry*, *266*(35), 23796–23801.

Ferrari, M., Twayana, S., Marini, F., & Pellicioli, A. (2018). A qPCR-Based Protocol to Quantify DSB Resection. *Methods in molecular biology (Clifton, N.J.)*, *1672*, 119–129.

Finn, R. D., Coggill, P., Eberhardt, R. Y., Eddy, S. R., Mistry, J., Mitchell, A. L., … Bateman, A. (2016). The Pfam protein families database: towards a more sustainable future. *Nucleic acids research*, *44*(D1), D279–D285.

Fontana, G. A., Hess, D., Reinert, J. K., Mattarocci, S., Falquet, B., Klein, D., Shore, D., Thomä, N. H., & Rass, U. (2019). Rif1 S-acylation mediates DNA double-strand break repair at the inner nuclear membrane. Nature communications, 10(1), 2535.

Fontana, G. A., Reinert, J. K., Thomä, N. H., & Rass, U. (2018). Shepherding DNA ends: Rif1 protects telomeres and chromosome breaks. *Microbial cell (Graz, Austria)*, *5*(7), 327–343.

Gao, Y., Shang, Q., Li, W., Guo, W., Stojadinovic, A., Mannion, C., Man, Y. G., & Chen, T. (2020). Antibiotics for cancer treatment: A double-edged sword. *Journal of Cancer, 11*(17), 5135–5149.

Garcia, A., Cayla, X., Guergnon, J., Dessauge, F., Hospital, V., Rebollo, M. P., Fleischer, A., & Rebollo, A. (2003). Serine/threonine protein phosphatases PP1 and PP2A are key players in apoptosis. *Biochimie, 85*(8), 721–726.

Garzón, J., Ursich, S., Lopes, M., Hiraga, S. I., & Donaldson, A. D. (2019). Human RIF1-Protein Phosphatase 1 Prevents Degradation and Breakage of Nascent DNA on Replication Stalling. *Cell reports, 27*(9), 2558–2566.e4.

Gasmi, N., Jacques, P. E., Klimova, N., Guo, X., Ricciardi, A., Robert, F., & Turcotte, B. (2014). The switch from fermentation to respiration in Saccharomyces cerevisiae is regulated by the Ert1 transcriptional activator/repressor. *Genetics, 198*(2), 547-560.

Gnan, S., Flyamer, I. M., Klein, K. N., Castelli, E., Rapp, A., Maiser, A., … Buonomo, S. C. B. (2021). Nuclear organisation and replication timing are coupled through RIF1-PP1 interaction. *Nature communications, 12*(1), 2910.

Gnügge, R., & Symington, L. S. (2020). Efficient DNA double-strand break formation at single or multiple defined sites in the Saccharomyces cerevisiae genome. *Nucleic acids research, 48*(20), e115.

Gnügge, R., Liphardt, T., & Rudolf, F. (2016). A shuttle vector series for precise genetic engineering of Saccharomyces cerevisiae. *Yeast (Chichester, England)*, *33*(3), 83–98.

Goffeau, A., Barrell, B. G., Bussey, H., Davis, R. W., Dujon, B., Feldmann, H., … Oliver, S. G. (1996). Life with 6000 genes. *Science (New York, N.Y.)*, *274*(5287), 546–567.

Hada, M., & Georgakilas, A. G. (2008). Formation of clustered DNA damage after high-LET irradiation: a review. *Journal of radiation research*, *49*(3), 203–210.

Hall, C., Brachat, S., & Dietrich, F. S. (2005). Contribution of horizontal gene transfer to the evolution of Saccharomyces cerevisiae. *Eukaryotic Cell*, *4*(6), 1102-1115.

Hartwell, L. H., Szankasi, P., Roberts, C. J., Murray, A. W., & Friend, S. H. (1997). Integrating genetic approaches into the discovery of anticancer drugs. *Science (New York, N.Y.)*, *278*(5340), 1064–1068.

Hiraga, S., Alvino, G. M., Chang, F., Lian, H. Y., Sridhar, A., Kubota, T., Brewer, B. J., Weinreich, M., Raghuraman, M. K., & Donaldson, A. D. (2014). Rif1 controls DNA replication by directing Protein Phosphatase 1 to reverse Cdc7-mediated phosphorylation of the MCM complex. *Genes & development*, *28*(4), 372–383.

Hiraga, S. I., Ly, T., Garzón, J., Hořejší, Z., Ohkubo, Y. N., Endo, A., Obuse, C., Boulton, S. J., Lamond, A. I., & Donaldson, A. D. (2017). Human RIF1 and protein phosphatase 1 stimulate DNA replication origin licensing but suppress origin activation. *EMBO reports*, *18*(3), 403–419.

Hurley, T. D., Yang, J., Zhang, L., Goodwin, K. D., Zou, Q., Cortese, M., Dunker, A. K., & DePaoli-Roach, A. A. (2007). Structural basis for regulation of protein phosphatase 1 by inhibitor-2. *The Journal of biological chemistry*, *282*(39), 28874–28883.

Isobe, S. Y., Hiraga, S. I., Nagao, K., Sasanuma, H., Donaldson, A. D., & Obuse, C. (2021). Protein phosphatase 1 acts as a RIF1 effector to suppress DSB resection prior to Shieldin action. *Cell reports*, *36*(2), 109383.

Jiang, Q., Lin. L., & Wang, T. (2008). A new model for apoptosis research: Yeast. *Progress in Biochemistry and Biophysics, 35,* 361.

Karathia, H., Vilaprinyo, E., Sorribas, A., & Alves, R. (2011). Saccharomyces cerevisiae as a model organism: a comparative study. *PLoS One, 6*(2), e16015.

Kedziora, S., Gali, V. K., Wilson, R. H. C., Clark, K. R. M., Nieduszynski, C. A., Hiraga, S. I., & Donaldson, A. D. (2018). Rif1 acts through Protein Phosphatase 1 but independent of replication timing to suppress telomere extension in budding yeast. *Nucleic acids research*, *46*(8), 3993–4003.

Knop, M. (2006). Evolution of the hemiascomycete yeasts: on life styles and the importance of inbreeding. *Bioessays, 28*(7), 696-708.

Koy, J. F., Pleninger, P., Wall, L., Pramanik, A., Martinez, M., & Moore, C. W. (1995). Genetic changes and bioassays in bleomycin- and phleomycin-treated cells, and their relationship to chromosomal breaks. *Mutation research*, *336*(1), 19–27.

Krol, K., Brozda, I., Skoneczny, M., Bretner, M., & Skoneczna, A. (2015). A genomic screen revealing the importance of vesicular trafficking pathways in genome maintenance and protection against genotoxic stress in diploid Saccharomyces cerevisiae cells. *PloS one*, *10*(3), e0120702.

Kross, J., Henner, W. D., Hecht, S. M., & Haseltine, W. A. (1982). Specificity of deoxyribonucleic acid cleavage by bleomycin, phleomycin, and tallysomycin. *Biochemistry*, *21*(18), 4310–4318.

Kumar, R., & Cheok, C. F. (2014). RIF1: a novel regulatory factor for DNA replication and DNA damage response signaling. *DNA repair*, *15*, 54–59.

Küntziger, T., Rogne, M., Folstad, R. L., & Collas, P. (2006). Association of PP1 with its regulatory subunit AKAP149 is regulated by serine phosphorylation flanking the RVXF motif of AKAP149. *Biochemistry*, *45*(18), 5868–5877.

Larasati (2020). The characterization of Dbf4 interactions and roles in genome replication and stability in Saccharomyces cerevisiae. UWSpace.

Laughery, M. F., Hunter, T., Brown, A., Hoopes, J., Ostbye, T., Shumaker, T., & Wyrick, J. J. (2015). New vectors for simple and streamlined CRISPR-Cas9 genome editing in Saccharomyces cerevisiae. *Yeast (Chichester, England)*, *32*(12), 711–720.

Lew, D. J., & Reed, S. I. (1995). A cell cycle checkpoint monitors cell morphogenesis in budding yeast. *The Journal of Cell Biology*, *129*(3), 739-749.

Li, H. J., Haque, Z. K., Chen, A., & Mendelsohn, M. (2007). RIF-1, a novel nuclear receptor corepressor that associates with the nuclear matrix. *Journal of cellular biochemistry*, *102*(4), 1021–1035.

Li, X., & Cai, M. (1997). Inactivation of the cyclin-dependent kinase Cdc28 abrogates cell cycle arrest induced by DNA damage and disassembly of mitotic spindles in Saccharomyces cerevisiae. *Molecular and Cellular Biology*, *17*(5), 2723-2734.

Liu, W., Li, L., Ye, H., Chen, H., Shen, W., Zhong, Y., Tian, T., & He, H. (2017). From *Saccharomyces cerevisiae* to human: The important gene co-expression modules. *Biomedical Reports*, *7*(2), 153-158.

Logan, M. R., Nguyen, T., Szapiel, N., Knockleby, J., Por, H., Zadworny, M., … Lesage, G. (2008). Genetic interaction network of the Saccharomyces cerevisiae type 1 phosphatase Glc7. *BMC genomics*, *9*, 336.

Matos, B., Howl, J., Jerónimo, C., & Fardilha, M. (2021). Modulation of serine/threonine-protein phosphatase 1 (PP1) complexes: A promising approach in cancer treatment. *Drug discovery today*, *26*(11), 2680–2698.

Mattarocci, S., Reinert, J. K., Bunker, R. D., Fontana, G. A., Shi, T., Klein, D., … Rass, U. (2017). Rif1 maintains telomeres and mediates DNA repair by encasing DNA ends. *Nature structural & molecular biology*, *24*(7), 588–595.

Mattarocci, S., Shyian, M., Lemmens, L., Damay, P., Altintas, D. M., Shi, T., Bartholomew, C. R., Thomä, N. H., Hardy, C. F., & Shore, D. (2014). Rif1 controls DNA replication timing in yeast through the PP1 phosphatase Glc7. *Cell reports*, *7*(1), 62–69.

Mei, Y., Liu, Y. B., Cao, S., Tian, Z. W., & Zhou, H. H. (2018). RIF1 promotes tumor growth and cancer stem cell-like traits in NSCLC by protein phosphatase 1-mediated activation of Wnt/β-catenin signaling. *Cell death & disease*, *9*(10), 942.

Mei, Y., Liu, Y. B., Hu, D. L., & Zhou, H. H. (2018). Effect of RIF1 on response of non-small-cell lung cancer patients to platinum-based chemotherapy by regulating MYC signaling pathway. *International journal of biological sciences*, *14*(13), 1859–1872.

Mei, Y., Peng, C., Liu, Y. B., Wang, J., & Zhou, H. H. (2017). Silencing RIF1 decreases cell growth, migration and increases cisplatin sensitivity of human cervical cancer cells. *Oncotarget*, *8*(63), 107044–107051.

Mendenhall, M. D., & Hodge, A. E. (1998). Regulation of Cdc28 cyclin-dependent protein kinase activity during the cell cycle of the yeast Saccharomyces cerevisiae. *Microbiology and molecular biology reviews : MMBR, 62*(4), 1191–1243.

Mohammadi, S., Saberidokht, B., Subramaniam, S. *et al.* (2015). Scope and limitations of yeast as a model organism for studying human tissue-specific pathways. *BMC Systems Biology, 9,* 96.

Møldrup, M. E., Salomonsen, B., & Halkier, B. A. (2012). Engineering of glucosinolate biosynthesis: candidate gene identification and validation. *Methods in enzymology, 515*, 291–313.

Monerawela C, Hiraga S, Donaldson AD. (2020). Checkpoint phosphorylation sites on budding yeast Rif1 protect nascent DNA from degradation by Sgs1-Dna2. bioRxiv. 10.1101/2020.06.25.170571.

Moore C. W. (1982). Control of in vivo (cellular) phleomycin sensitivity by nuclear genotype, growth phase, and metal ions. *Cancer research, 42*(3), 929–933.

Moore C. W. (1988). Internucleosomal cleavage and chromosomal degradation by bleomycin and phleomycin in yeast. *Cancer research, 48*(23), 6837–6843.

Mukherjee, C., Tripathi, V., Manolika, E. M., Heijink, A. M., Ricci, G., Merzouk, S., de Boer, H. R., Demmers, J., van Vugt, M. A. T. M., & Ray Chaudhuri, A. (2019). RIF1 promotes replication fork protection and efficient restart to maintain genome stability. *Nature communications, 10*(1), 3287.

O'Connell, K., Jinks-Robertson, S., & Petes, T. D. (2015). Elevated Genome-Wide Instability in Yeast Mutants Lacking RNase H Activity. *Genetics*, *201*(3), 963–975.

O'Farrell P. H. (2011). Quiescence: early evolutionary origins and universality do not imply uniformity. *Philosophical transactions of the Royal Society of London. Series B, Biological sciences*, *366*(1584), 3498–3507.

Parapouli, M., Vasileiadis, A., Afendra, A. S., & Hatziloukas, E. (2020). *Saccharomyces cerevisiae* and its industrial applications. *AIMS Microbiology*, *6*(1), 1-31.

Peng, Z. Y., Trumbly, R. J., & Reimann, E. M. (1990). Purification and characterization of glycogen synthase from a glycogen-deficient strain of Saccharomyces cerevisiae. *The Journal of biological chemistry*, *265*(23), 13871–13877.

Petering, D. H., Byrnes, R. W., & Antholine, W. E. (1990). The role of redox-active metals in the mechanism of action of bleomycin. *Chemico-biological interactions*, *73*(2-3), 133–182.

Peti, W., Nairn, A. C., & Page, R. (2013). Structural basis for protein phosphatase 1 regulation and specificity. *The FEBS journal*, *280*(2), 596–611.

Povirk, L. F., Hogan, M., Dattagupta, N., & Buechner, M. (1981). Copper(II).bleomycin, iron(III).bleomycin, and copper(II).phleomycin: comparative study of deoxyribonucleic acid binding. *Biochemistry*, *20*(3), 665–671.

Prakash, R., Zhang, Y., Feng, W., & Jasin, M. (2015). Homologous recombination and human health: the roles of BRCA1, BRCA2, and associated proteins. *Cold Spring Harbor perspectives in biology*, *7*(4), a016600.

Ramotar, D., & Masson, J. Y. (1996). Saccharomyces cerevisiae DNA repair processes: an update. *Molecular and Cellular Biochemistry*, *58*(1), 65-75.

Reiter, H., Milewskiy, M., & Kelley, P. (1972). Mode of action of phleomycin on Bacillus subtilis. *Journal of bacteriology*, *111*(2), 586–592.

Rojas, M., Gingras, A. C., & Dever, T. E. (2014). Protein phosphatase PP1/GLC7 interaction domain in yeast eIF2γ bypasses targeting subunit requirement for eIF2α dephosphorylation. *Proceedings of the National Academy of Sciences of the United States of America*, *111*(14), E1344–E1353.

Ross, E. M., & Maxwell, P. H. (2018). Low doses of DNA damaging agents extend Saccharomyces cerevisiae chronological lifespan by promoting entry into quiescence. *Experimental gerontology*, *108*, 189–200.

Sabourin, M., Nitiss, J. L., Nitiss, K. C., Tatebayashi, K., Ikeda, H., & Osheroff, N. (2003). Yeast recombination pathways triggered by topoisomerase II-mediated DNA breaks. *Nucleic acids research*, *31*(15), 4373–4384.

Sahaya Glingston, R., Yadav, J., Rajpoot, J., Joshi, N., & Nagotu, S. (2021). Contribution of yeast models to virus research. *Applied Microbiology and Biotechnology*, *105*(12), 4855–4878.

Seluanov, A., Mittelman, D., Pereira-Smith, O. M., Wilson, J. H., & Gorbunova, V. (2004). DNA end joining becomes less efficient and more error-prone during cellular senescence. *Proceedings of the National Academy of Sciences of the United States of America*, *101*(20), 7624–7629.

Sheng, H., Qi, L., Sui, Y., Li, Y. Z., Yu, L. Z., Zhang, K., Xu, J. Z., Wang, P. M., & Zheng, D. Q. (2019). Mapping chromosomal instability induced by small-molecular therapeutics in a yeast model. *Applied microbiology and biotechnology*, *103*(12), 4869–4880.

Shenolikar, S., & Nairn, A. C. (1991). Protein phosphatases: recent progress. *Advances in second messenger and phosphoprotein research*, *23*, 1–121.

Shubin, C. B., Mayangsari, R., Swett, A. D., & Greider, C. W. (2021). Rif1 regulates telomere length through conserved HEAT repeats. *Nucleic acids research*, *49*(7), 3967–3980.

Shyian, M., Mattarocci, S., Albert, B., Hafner, L., Lezaja, A., Costanzo, M., Boone, C., & Shore, D. (2016). Budding Yeast Rif1 Controls Genome Integrity by Inhibiting rDNA Replication. PLoS Genet. 12(11):e1006414.

Silverman, J., Takai, H., Buonomo, S. B., Eisenhaber, F., & de Lange, T. (2004). Human Rif1, ortholog of a yeast telomeric protein, is regulated by ATM and 53BP1 and functions in the S-phase checkpoint. *Genes & development*, *18*(17), 2108–2119.

Spitzner, J. R., Chung, I. K., Gootz, T. D., McGuirk, P. R., & Muller, M. T. (1995). Analysis of eukaryotic topoisomerase II cleavage sites in the presence of the quinolone CP-115,953 reveals drug-dependent and -independent recognition elements. *Molecular pharmacology*, *48*(2), 238–249.

Sreesankar, E., Senthilkumar, R., Bharathi, V., Mishra, R.K., & Mishra, K. (2012). Functional diversification of yeast telomere associated protein, Rif1, in higher eukaryotes. *BMC Genomics, 13,* 255.

Stokowa-Sołtys, K., Dzyhovskyi, V., Wieczorek, R., & Jeżowska-Bojczuk, M. (2019). Phleomycin complex - Coordination mode and in vitro cleavage of DNA. *Journal of inorganic biochemistry*, *195*, 71–82.

Strecker, J., Gupta, G. D., Zhang, W., Bashkurov, M., Landry, M. C., Pelletier, L., & Durocher, D. (2016). DNA damage signalling targets the kinetochore to promote chromatin mobility. *Nature cell biology*, *18*(3), 281–290.

Sun, S., & Gresham, D. (2021). Cellular quiescence in budding yeast. *Yeast (Chichester, England)*, *38*(1), 12–29.

Sung, H., Ferlay, J., Siegel, R. L., Laversanne, M., Soerjomataram, I., Jemal, A., & Bray, F. (2021). Global Cancer Statistics 2020: GLOBOCAN Estimates of Incidence and Mortality

Worldwide for 36 Cancers in 185 Countries. *CA: a cancer journal for clinicians*, *71*(3), 209–249.

Takata, M., Sasaki, M. S., Sonoda, E., Morrison, C., Hashimoto, M., Utsumi, H., Yamaguchi-Iwai, Y., Shinohara, A., & Takeda, S. (1998). Homologous recombination and non-homologous end-joining pathways of DNA double-strand break repair have overlapping roles in the maintenance of chromosomal integrity in vertebrate cells. *The EMBO journal*, *17*(18), 5497–5508.

Tanaka, S., Nakato, R., Katou, Y., Shirahige, K., & Araki, H. (2011). Origin association of Sld3, Sld7, and Cdc45 proteins is a key step for determination of origin-firing timing. *Current biology : CB*, *21*(24), 2055–2063.

Tanaka, S., Umemori, T., Hirai, K., Muramatsu, S., Kamimura, Y., & Araki, H. (2007). CDK-dependent phosphorylation of Sld2 and Sld3 initiates DNA replication in budding yeast. *Nature*, *445*(7125), 328–332.

Terrak, M., Kerff, F., Langsetmo, K., Tao, T., & Dominguez, R. (2004). Structural basis of protein phosphatase 1 regulation. *Nature*, *429*(6993), 780–784.

Tu, J., & Carlson, M. (1995). REG1 binds to protein phosphatase type 1 and regulates glucose repression in Saccharomyces cerevisiae. *The EMBO journal*, *14*(23), 5939–5946.

Valcourt, J. R., Lemons, J. M., Haley, E. M., Kojima, M., Demuren, O. O., & Coller, H. A. (2012). Staying alive: metabolic adaptations to quiescence. *Cell cycle (Georgetown, Tex.), 11*(9), 1680–1696.

Verdugo-Sivianes, E. M., Navas, L., Molina-Pinelo, S., Ferrer, I., Quintanal-Villalonga, A., Peinado, J., … Carnero, A. (2017). Coordinated downregulation of Spinophilin and the catalytic subunits of PP1, PPP1CA/B/C, contributes to a worse prognosis in lung cancer. *Oncotarget*, *8*(62), 105196–105210.

Wood, V., Rutherford, K. M., Ivens, A., Rajandream, M. A., & Barrell, B. (2001). A re-annotation of the Saccharomyces cerevisiae genome. *Comparative and Functional Genomics, 2*(3), 143-154.

Wu, X., Hart, H., Cheng, C., Roach, P. J., & Tatchell, K. (2001). Characterization of Gac1p, a regulatory subunit of protein phosphatase type I involved in glycogen accumulation in Saccharomyces cerevisiae. *Molecular genetics and genomics : MGG*, *265*(4), 622–635.

Xu, L., & Blackburn, E. H. (2004). Human Rif1 protein binds aberrant telomeres and aligns along anaphase midzone microtubules. *The Journal of cell biology*, *167*(5), 819–830.

Yan, L., Rosen, N., & Arteaga, C. (2011). Targeted cancer therapies. *Chinese journal of cancer*, *30*(1), 1–4.

Zeman, M. K., & Cimprich, K. A. (2014). Causes and consequences of replication stress. *Nature cell biology*, *16*(1), 2–9.

Zhong, Z., Shiue, L., Kaplan, S., & de Lange, T. (1992). A mammalian factor that binds telomeric TTAGGG repeats in vitro. *Molecular and cellular biology*, *12*(11), 4834–4843.

Zhou, B. B., & Elledge, S. J. (2000). The DNA damage response: putting checkpoints in perspective. *Nature*, *408*(6811), 433–439.

Zhu, Y. O., Siegal, M. L., Hall, D. W., & Petrov, D. A. (2014). Precise estimates of mutation rate and spectrum in yeast. *Proceedings of the National Academy of Sciences of the United States of America*, *111*(22), E2310–E2318.

Zimmermann, M., Lottersberger, F., Buonomo, S. B., Sfeir, A., & de Lange, T. (2013). 53BP1 regulates DSB repair using Rif1 to control 5' end resection. *Science (New York, N.Y.)*, *339*(6120), 700–704.